PERGAMON

Journal of Structural Geology 25 (2003) 1933–1957

JOURNAL OF STRUCTURAL GEOLOGY

www.elsevier.com/locate/jsg

Structure, emplacement and lateral expansion of the San José tonalite pluton, Peninsular Ranges batholith, Baja California, México

S.E. Johnson[a,*], J.M. Fletcher[b], C.M. Fanning[c], R.H. Vernon[d,e], S.R. Paterson[e], M.C. Tate[d]

[a]*Department of Geological Sciences, University of Maine, Orono, ME 04469-5790, USA*
[b]*Departamento de Geologia, CICESE, Km 107 Carratera Ensenada-Tijuana, Baja California, México*
[c]*Research School of Earth Sciences, Australian National University, Canberra, ACT 0200, Australia*
[d]*Department of Earth and Planetary Sciences, and Key Centre for the GEMOC, Macquarie University, Sydney, New South Wales 2109, Australia*
[e]*Department of Earth Sciences, University of Southern California, Los Angeles, CA 90089-0740, USA*

Received 8 May 2001; received in revised form 15 November 2002; accepted 17 January 2003

Abstract

The 108 km^2 San José pluton forms part of the Jurassic to Cretaceous Peninsular Ranges batholith of northern Baja California, México. The pluton was formed by three nested, southward-migrating intrusive pulses, and the internal contacts between them indicate juxtaposition while the adjoining pulses were magmas. SHRIMP U–Pb zircon data indicate that the entire pluton was emplaced in less than 4.4 m.y.; ages of the individual pulses cannot be separated at the 95% confidence interval, owing primarily to low uranium content of zircon. Detailed structural data and geologic mapping are consistent with a component of asymmetrical, lateral expansion at the site of emplacement. The direction of maximum lateral expansion may have been controlled by thermal, compositional and resulting rheological gradients in the surrounding wall rocks. A carapace of predominantly solid-state deformation marks the northern two-thirds of the pluton, and the early stages of this fabric may have formed in the presence of a small amount of melt. Lack of evidence for syn- to post-emplacement regional ductile deformation around the pluton suggests that this carapace was deformed during the lateral expansion of the pluton.

Keywords: Foliation development; Geochronology; Pluton Emplacement; Submagmatic flow; Subsolidus flow

1. Introduction

This paper examines the structure and emplacement history of the 108 km^2 San José tonalite pluton, located in the Sierra San Pedro Mártir region of northern Baja California, México (Figs. 1 and 2). The combination of excellent exposure, lack of evidence for post-emplacement regional deformation, and a detailed structural data set make the San José pluton an unusually good candidate for testing models of in-situ expansion. This paper emphasizes the importance of lineation data in both the pluton and surrounding country rocks for evaluating the kinematics of pluton ascent and emplacement.

The Jurassic to Cretaceous Peninsular Ranges batholith of northern Baja California, México, contains approximately 400 plutons of mainly tonalitic and granodioritic composition (Gastil et al., 1975), although gabbro is common in the western part of the batholith. Unlike the Sierra Nevada batholith to the north, many of these plutons are completely separated by an interconnected framework of country rocks, similar to the isolated plutons of the White–Inyo Range of eastern California (e.g. Bateman, 1992). In the western part of the batholith, the weakly metamorphosed volcanic, volcaniclastic and volcanogenic sedimentary country rocks appear to have been deformed by only one regional folding event and commonly contain lithic tuffs that are useful for finite strain analysis (Johnson et al., 1999a). For these reasons, combined with the commonly excellent exposure and access, this is an ideal region for studying the structural evolution of mid- to upper-crustal magma plumbing systems (e.g. Johnson et al., 1999a, b; Tate et al., 1999; Tate and Johnson, 2000).

The San José pluton has many characteristics in common with plutons exposed at middle- to upper-crustal levels throughout the world, including: (1) an elliptical shape with low aspect ratio (<2:1) in plan view; (2) multiple

* Corresponding author.
E-mail address: johnsons@maine.edu (S.E. Johnson).

0191-8141/03/$ - see front matter © 2003 Elsevier Ltd. All rights reserved.
doi:10.1016/S0191-8141(03)00015-4

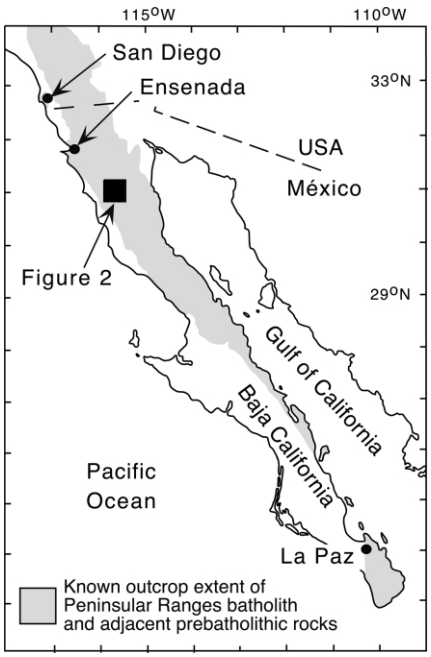

Fig. 1. Map showing the Baja California peninsula. The Peninsular Ranges batholith and adjacent prebatholithic country rocks are shaded.

sub-concentric intrusive phases; (3) a concentric, solid-state foliation along its margin, but mainly magmatic foliation in the interior; (4) gradients in magmatic foliation intensity, which generally increases towards the margins; (5) concordant contacts with compositional and deformational layering in wall rocks around much of the outer margin; and (6) strong deflection of wall rocks within a generally narrow deformation aureole. This characteristic suite of features is commonly interpreted to result from some process, or combination of processes, associated with the ascent, emplacement and crystallization of plutons including: (1) diapiric rise of magma (e.g. Schmeling et al., 1988; Cruden, 1990; Paterson and Vernon, 1995; Weinberg and Podladchikov, 1995; Miller and Paterson, 1999); (2) downward flow of aureole rocks to fill space around ascending plutons (e.g. Bridgewater et al., 1974; Saleeby, 1990; Stein and Paterson, 1996; Johnson et al., 1999a); (3) in-situ expansion or 'ballooning' of magma chambers (e.g. Nelson and Sylvester, 1971; Sylvester et al., 1978; Holder, 1979; Bateman, 1985; Courrioux, 1987; Ramsay, 1989); (4) regional deformation during and or after emplacement (e.g. Vernon and Paterson, 1993; Paterson and Vernon, 1995); (5) sinking of plutons that become denser than their surrounding country rocks following crystallization (e.g. Glazner, 1994; Weinberg and Podladchikov, 1995; Glazner and Miller, 1998; Johnson et al., 1999a), and (6) progressive depression of the pluton floor (Cruden, 1998; Wiebe and Collins, 1998). In this paper we present critical structural, microstructural, petrological, and relative and absolute chronological evidence in and around the San José pluton to evaluate the relative importance of these processes.

Unlike many other plutons with those features listed above, the San José pluton appears to postdate most or all of the regional deformation in surrounding country rocks, and so the solid-state foliation in the pluton's margin may have been caused by emplacement-related stresses, rather than syn- to post-emplacement regional deformation. The San José pluton appears to have undergone a component of lateral expansion at the site of emplacement, and our work shows that chamber expansion can be highly asymmetrical, owing to the inherent thermal and mechanical heterogeneity of the middle to upper crust.

2. Geological setting

The Jurassic to Cretaceous Peninsular Ranges batholith is one of the great Mesozoic batholiths of western North America, extending some 1600 km from southern California, USA, to the tip of Baja California, México (Fig. 1). The batholith is divisible into western and eastern belts on the basis of geologic, petrologic, geophysical, geochemical and isotopic gradients or discontinuities (Todd and Shaw, 1985; Silver and Chappell, 1988; Todd et al., 1988; Walawender et al., 1991; Thompson and Girty, 1994; Ichinose et al., 1996; Johnson et al., 1999b; Tate and Johnson, 2000). In northern Baja California, the western part of the batholith intruded Mesozoic volcanic-arc and basinal volcano-sedimentary assemblages, whereas the eastern part intruded Triassic to Cretaceous 'flysch' and Proterozoic to Paleozoic passive-margin sediments. Although interpretations vary, most previous workers have considered the boundary between these belts to be a suture between the North American craton and a fringing arc, which were originally separated by a back-arc basin (Gastil et al., 1978, 1981; Rangin, 1978; Phillips, 1993; Busby et al., 1998) or a basin of unspecified origin (Todd et al., 1988; Griffith and Hoobs, 1993). Alternatively, Walawender et al. (1991) and Thompson and Girty (1994) suggested that the batholith may have formed in-situ across a poorly understood, pre-Triassic boundary between oceanic and continental crust. Johnson et al. (1999b) described a major ductile thrust (Main Mártir Thrust), which they interpreted as part of a broad suture zone between the eastern and western portions of the batholith (Fig. 2). This thrust is coincident, in the area of Fig. 2, with the boundary between the eastern and western PRB proposed by Gastil et al. (1975). However, we are not certain whether the thrust corresponds with Gastil's boundary in other parts of the batholith to the north and south, and this remains a subject of investigation by different research groups. On the basis of work conducted in the area of Fig. 2; Johnson et al. (1999b) suggested that an island arc (Alisitos arc) collided with the North American margin approximately 110 Ma. In their model this collision caused substantial crustal thickening near the boundary between the two crustal blocks, and this thickened zone was stitched by numerous tonalite plutons, one of which is the San José pluton, between ca. 110 and 100 Ma.

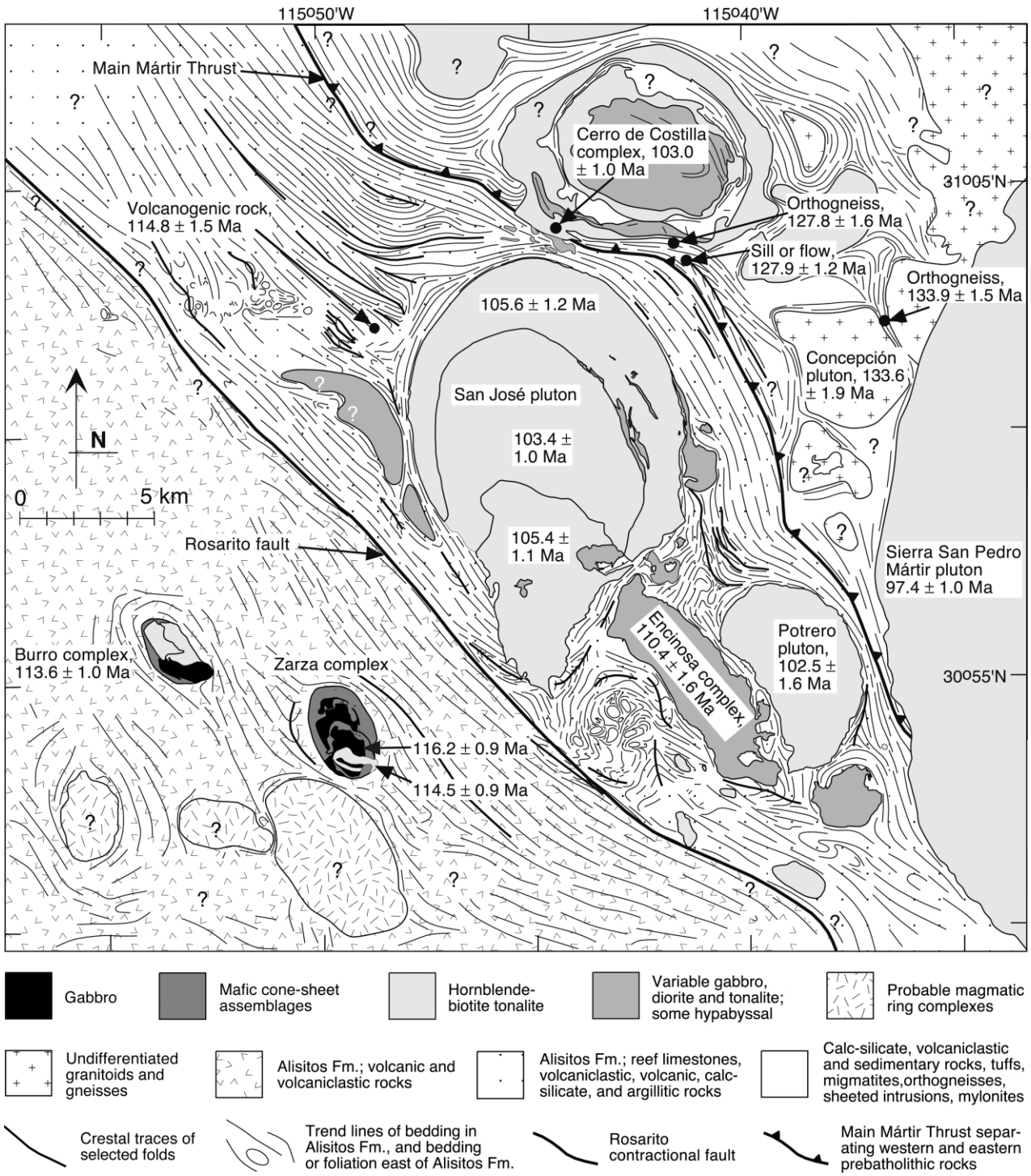

Fig. 2. Geological map of the area identified in Fig. 1. Map constructed from a combination of detailed ground mapping and air photo interpretation. Question marks indicate general areas that have not been ground checked and/or where the air photos were unclear. All ages are from SHRIMP U–Pb zircon data; data not presented here was reported in Johnson et al. (1999b). See the legend for location and geologic information. The San José pluton is located in the center of the map.

3. The San José pluton

The San José pluton consists of three distinct units, which we describe below in terms of rock types, intrusive relationships, structures, microstructures, kinematics, and SHRIMP U–Pb chronology. Figures. 2–5 show the geology, bedding/foliation data and lineation data, respectively, in the pluton and surrounding country rocks. Figures. 6 and 7 show trend analyses for the bedding/foliation and lineation data. Figures. 8 and 9 show block diagrams along the cross-section lines shown in Fig. 6.

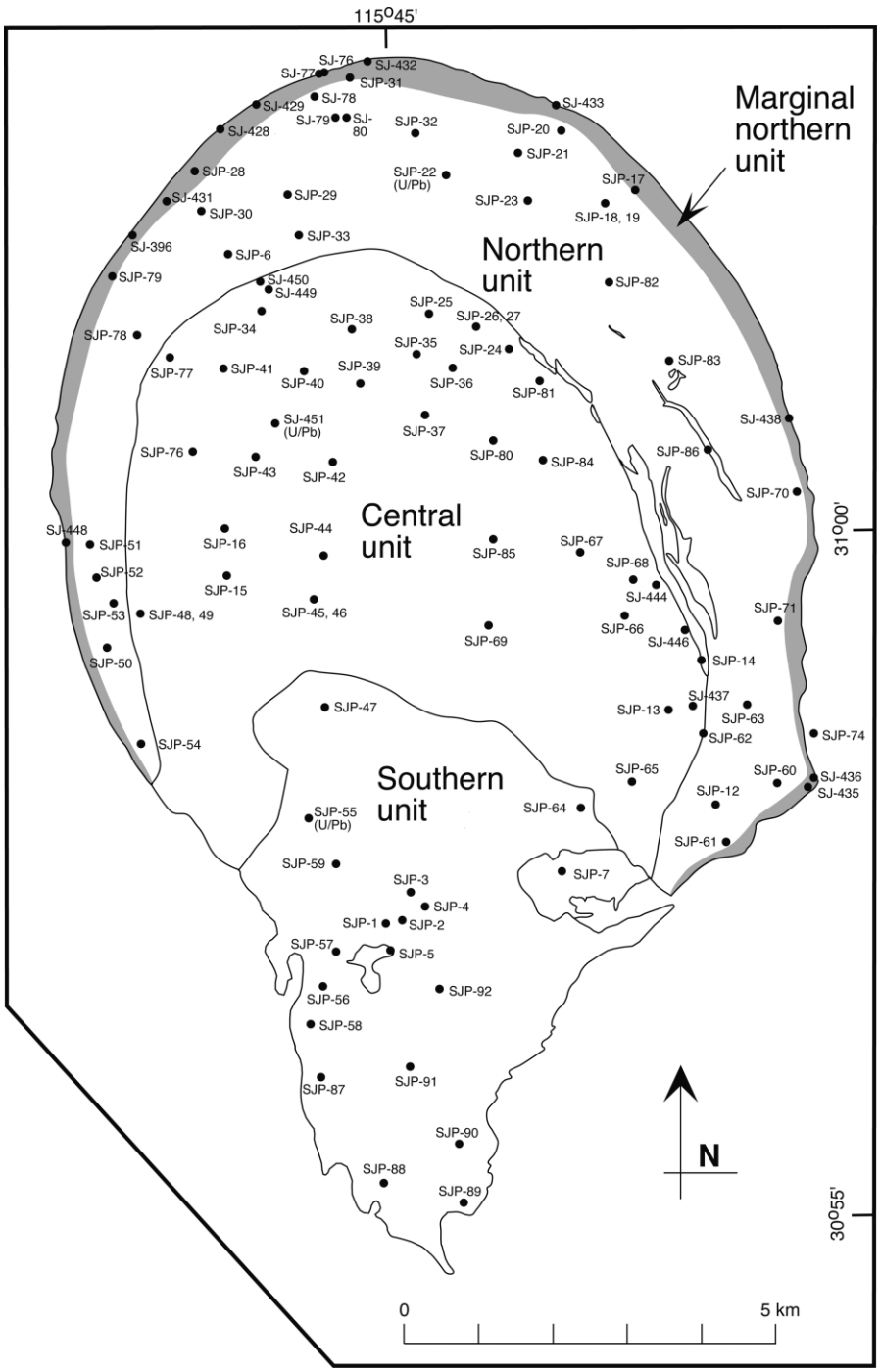

Fig. 3. Map identifying the three textural units of the San José pluton: northern unit = stubby hornblende tonalite; central unit = prismatic hornblende tonalite; southern unit = seriate porphyritic tonalite; marginal northern unit = gneissic border-phase tonalite (outer margin of the northern unit), within which the pluton shows an appreciable outward-increasing solid-state deformation gradient. Black dots show locations where 102 samples were collected.

Murray (1978) made a very detailed study of the pluton, and although we have remapped his entire study area, we have used many of his foliation and lineation measurements within the pluton and in the wall rocks immediately adjacent to it. Owing to the detailed description of the pluton by Murray (1978), some of our descriptive material below summarizes his findings.

Fig. 4. Map showing bedding and foliation data within and surrounding the San José pluton. Approximately 2200 measurements. Data from principle author, Murray (1978) and Chavez (1998).

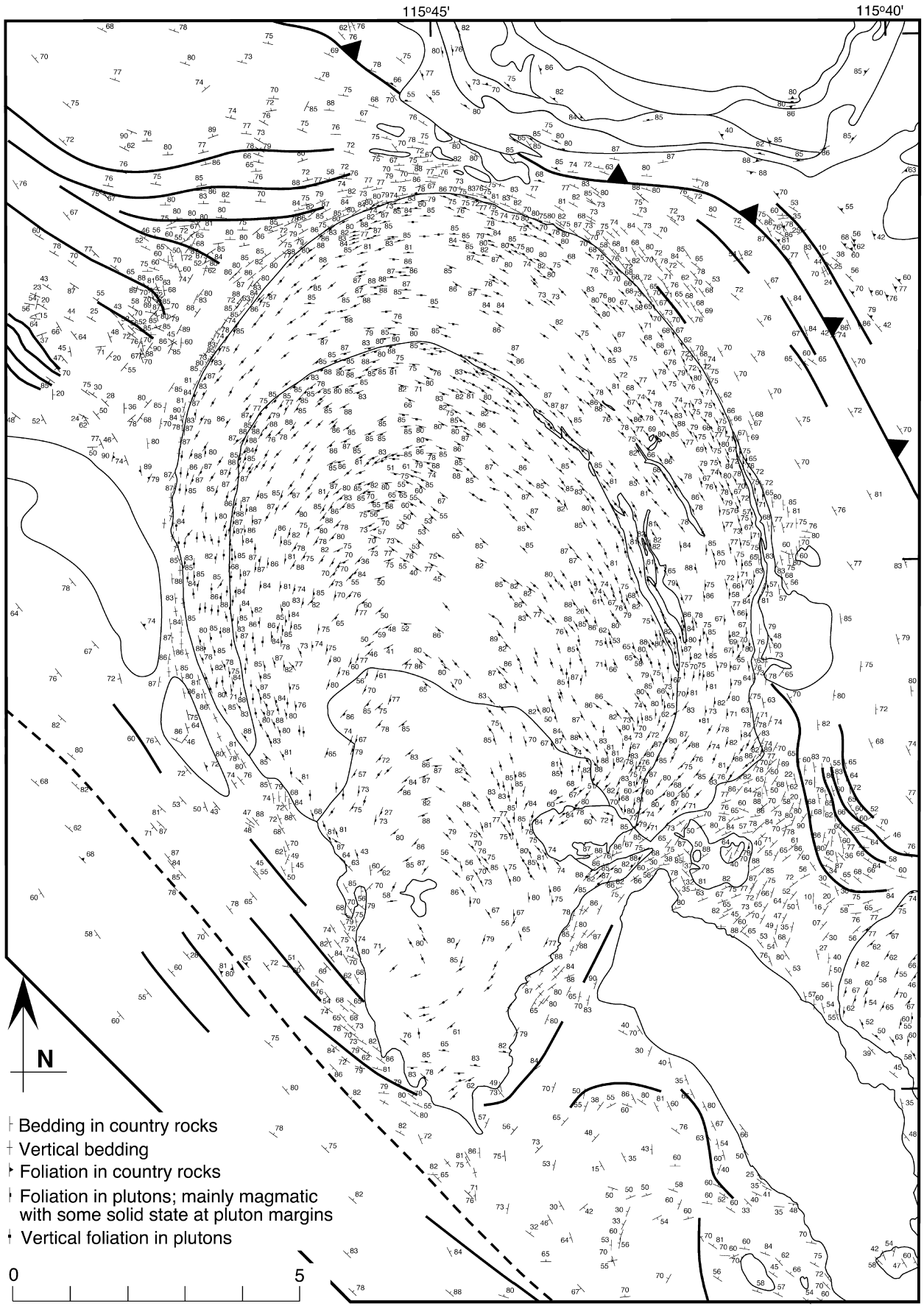
115°45'
115°40'
31°05'
31°00'
30°55'
N
Bedding in country rocks
Vertical bedding
Foliation in country rocks
Foliation in plutons; mainly magmatic with some solid state at pluton margins
Vertical foliation in plutons
0
5

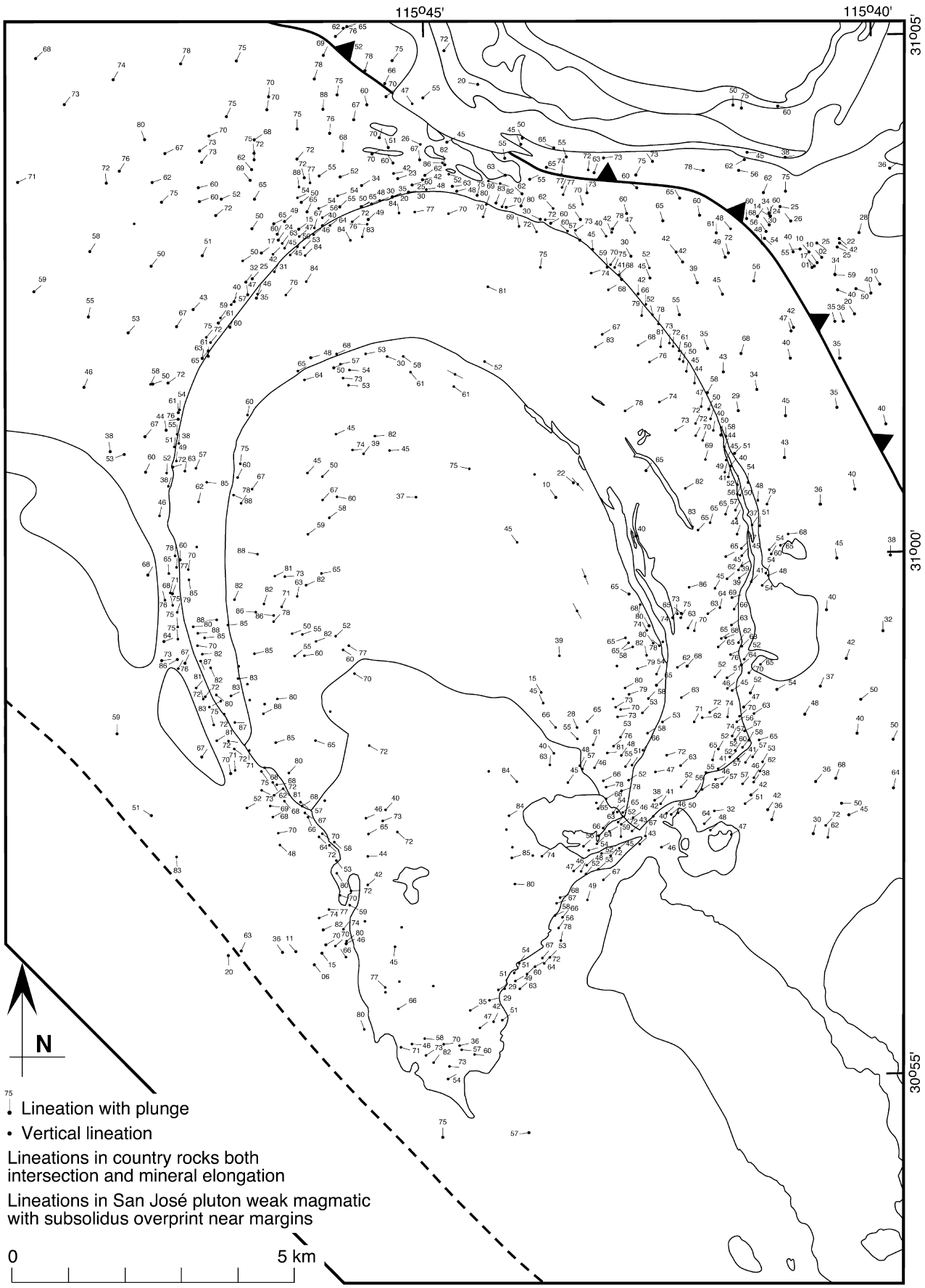
115°45'
115°40'
31°05'
31°00'
30°55'
N
Lineation with plunge
Vertical lineation
Lineations in country rocks both intersection and mineral elongation
Lineations in San José pluton weak magmatic with subsolidus overprint near margins
0
5 km

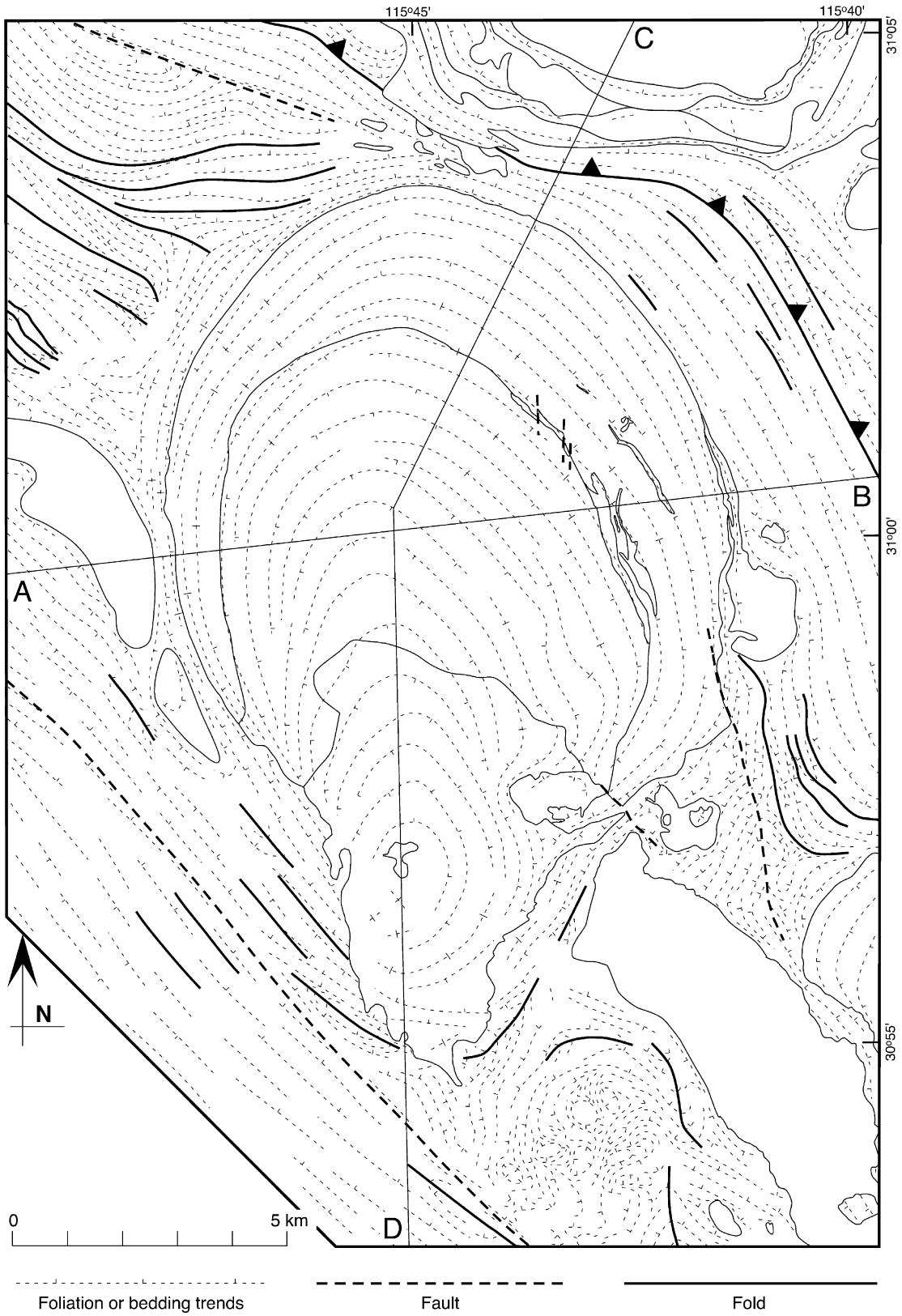

Fig. 6. Composite map of foliation and bedding trends, folds and faults within and surrounding the San José pluton. Block-diagram cross-sections along the lines A–B and C–D are shown in Figs. 8 and 9, respectively.

Fig. 5. Map showing lineation data within and surrounding the San José pluton. Approximately 770 measurements. Data from principle author and Murray (1978).

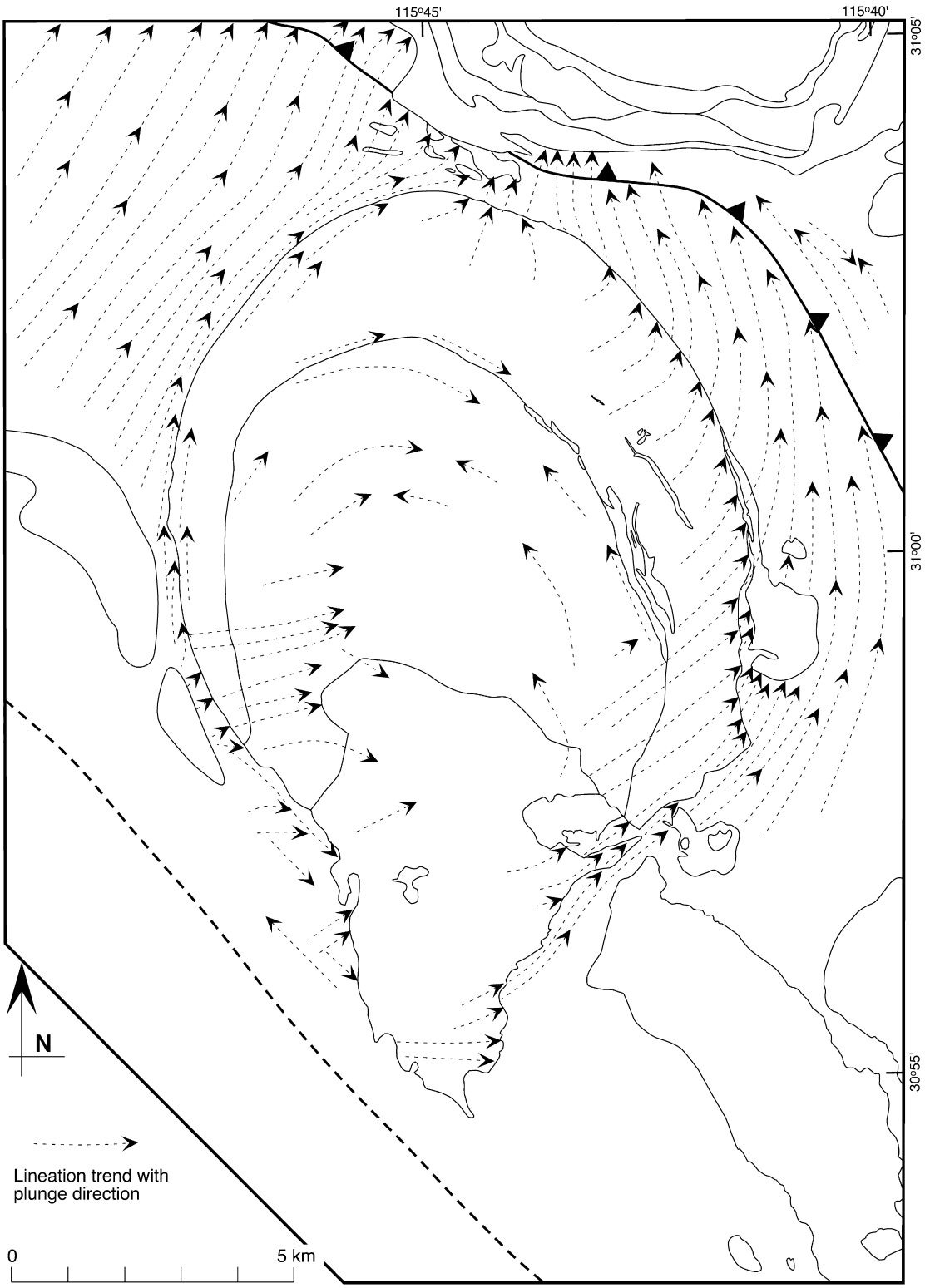

Fig. 7. Composite map of lineation trends within and surrounding the San José pluton.

3.1. General description and rock types

More than 95% of the bimodal San José pluton is composed of distinctive, homogeneous, coarse-grained (>3.0 mm), white-weathering, hornblende–biotite tonalite with abundant microgranitoid enclaves (~1%) and rare wall-rock xenoliths. The remaining 4–5% of the body is composed of largely synplutonic, hornblende-bearing sheets, dikes and elliptical intrusions of intermediate to mafic composition, some of which are localized along

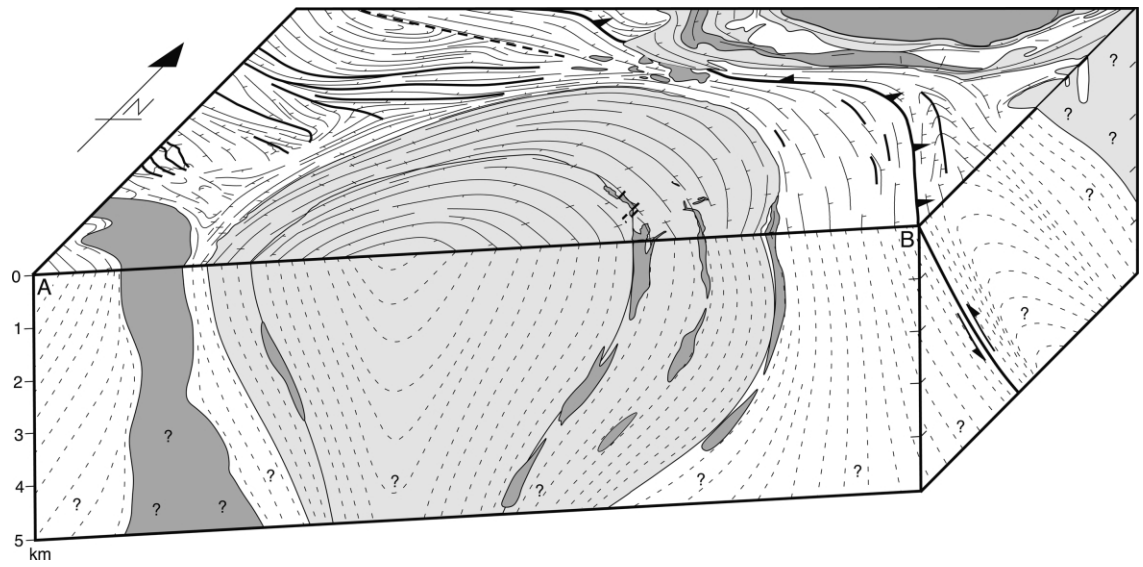

Fig. 8. Block-diagram cross-section along the line A–B in Fig. 6. See Fig. 2 for geology legend. Vertical and horizontal scales are equal.

internal contacts within the pluton (Figs. 2 and 3). Swarms of microgranitoid enclaves have similar compositions to these intermediate to mafic rocks (Tate and Johnson, 2000), and their abundance indicates widespread magma mingling. Enclave features indicative of mingling include pillow-like, lobate shapes with crenulate, chilled margins (e.g. Vernon et al., 1988). On the basis of texture and general outcrop appearance, Murray (1978) divided the pluton into three discrete tonalite units (Fig. 3). From north to south, these are: (1) stubby hornblende tonalite (referred to as *northern unit* here), which is characterized by stubby, relatively equant hornblende and equigranular texture; (2) prismatic hornblende tonalite (referred to as *central unit* here), which has a 'seriate' texture characterized by prismatic hornblende and thin biotite plates; and (3) seriate porphyritic tonalite (referred to as *southern unit* here), which is identical to the central unit with the addition of sparse (<0.5%), euhedral plagioclase phenocrysts up to 15–20 mm long. Murray (1978) further subdivided the outer margin of the northern unit into a gneissose border-phase tonalite (referred to as *marginal northern unit* here), characterized by solid-state deformation fabrics that overprint pre-existing magmatic ones (discussed further below).

As noted by Murray (1978), the tonalite units are chemically very homogeneous, with a total SiO_2 range of 59.4–65.2%. They are also extremely calcic (alkali–lime index = 63) and extremely low in K_2O (average = 0.74%). The pluton is peraluminous (A/CNK > 1.1), and initial Sr compositions (0.7035 ± 6) and ϵ_{Nd} values (4.85 ± 0.05) (Tate and Johnson, 2000) are primitive relative to the compositional field for the batholith (DePaolo, 1981).

The average mode of the tonalites is $Plg_{64}Hbe_{11}Bt_{5-6}Qtz_{16}Opq_{0.3}$, and K-feldspar makes up less than 0.3% (Murray, 1978). Biotite modes in the marginal northern unit are as high as 10% (Murray, 1978). Plagioclase and hornblende compositions (S.E. Johnson, unpublished data)

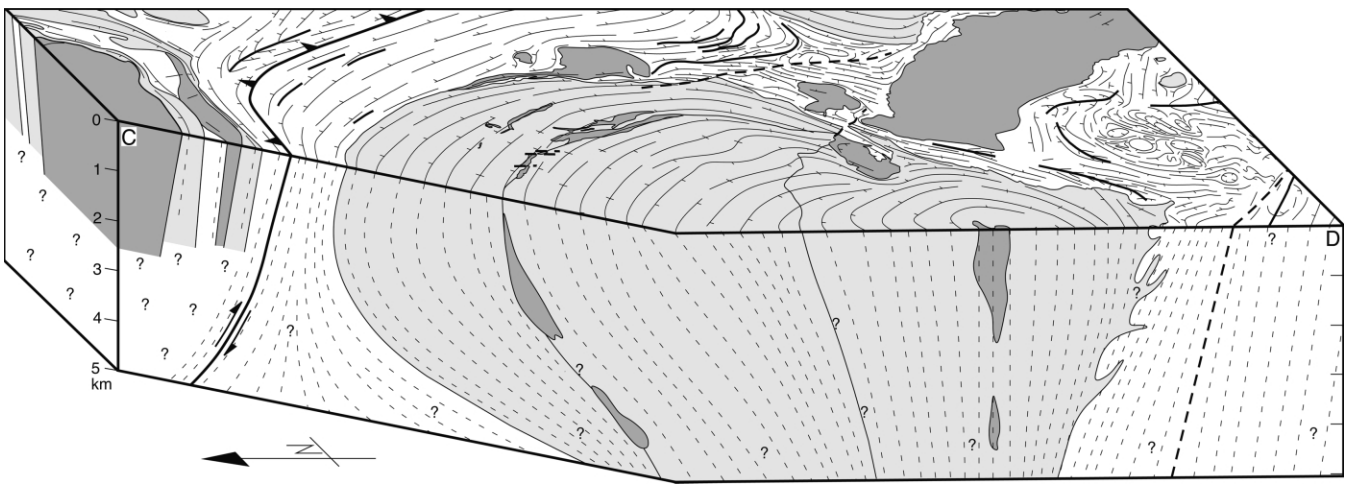

Fig. 9. Block-diagram cross-section along the line C–D in Fig. 6. See Fig. 2 for geology legend. Vertical and horizontal scales are equal.

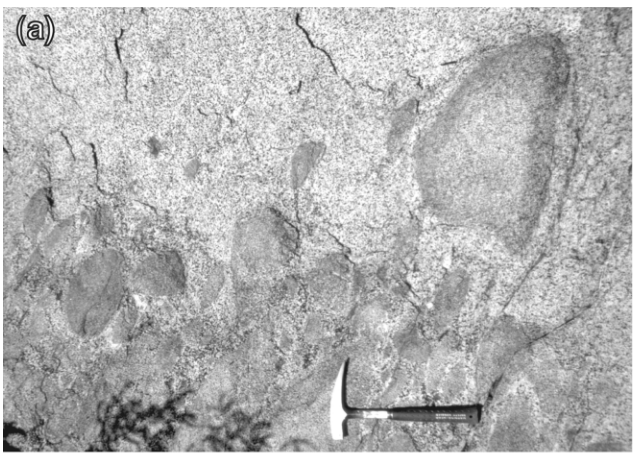
(a)

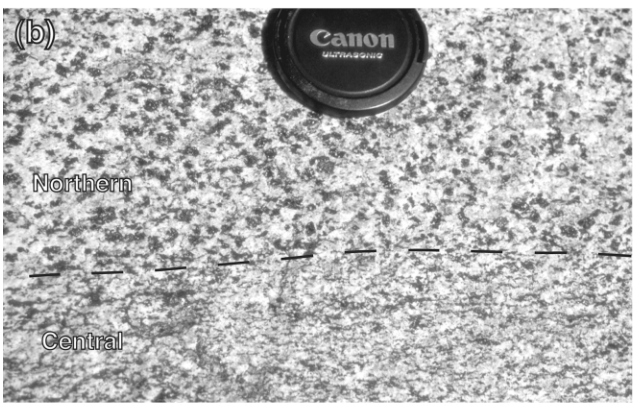
(b)
Canon
Northern
Central

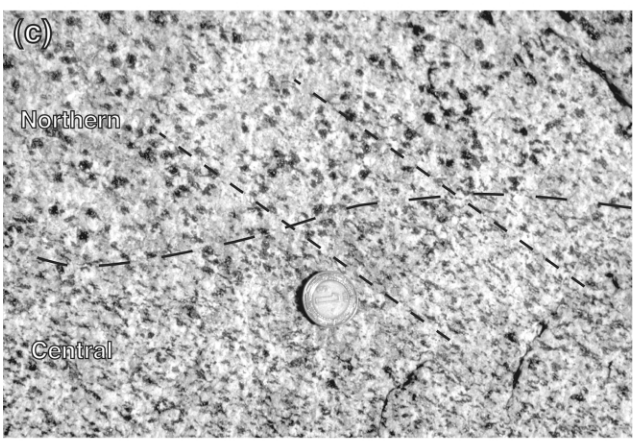
(c)
Northern
Central


(d)

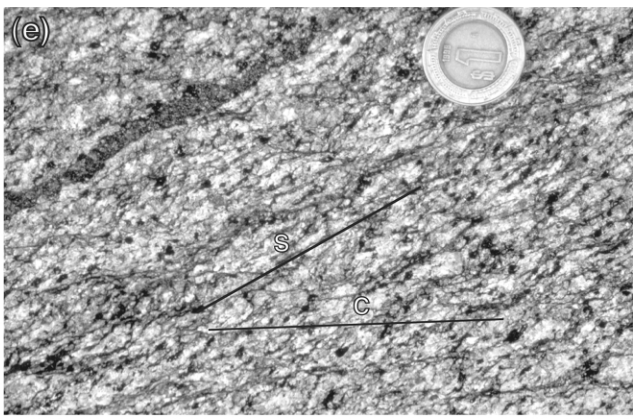
(e)
S
C

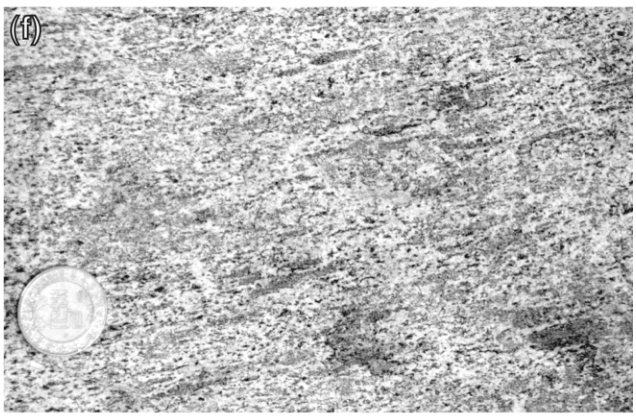
(f)


(g)

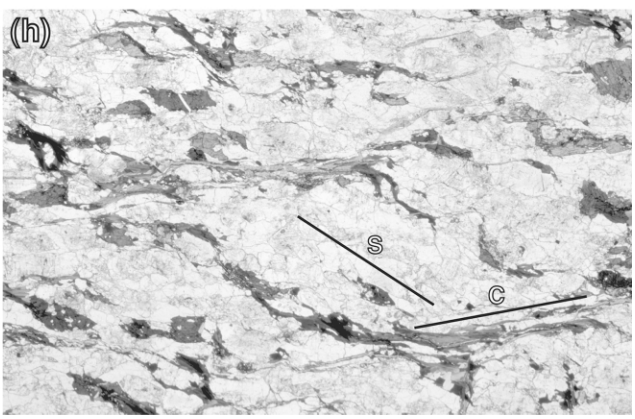
(h)
S
C

closely resemble those in the Zarza Intrusive Complex to the southwest (Johnson et al., 1999a), and so suggest similar emplacement pressures of ca. 2.3 ± 0.6 kbar.

3.2. Internal contact relationships between tonalite units

3.2.1. Contact between northern and central units

This contact is gradational across a zone ranging in width from 2 to 100 m, and the two units are separated by sheets of intermediate to mafic composition for approximately 6 km in the eastern part of the pluton (Figs. 2 and 3). These sheets are synplutonic, as indicated by intricate mingling relationships with both tonalite units, as well as pillows of microgranitoid enclaves emanating from some of their margins (Fig. 10a). The contact is narrowest to the north, where it appears in places to separate the two tonalite units over no more than 2 or 3 m, and progressively widens to 100 m at its southwestern and southeastern terminations. Murray (1978) originally mapped this gradational contact as separating areas containing typical northern unit tonalite (with or without central unit tonalite) from areas containing only central unit tonalite, and we have retained his contact on our maps.

The two tonalite units are intimately interlayered and mutually intrusive at many outcrops, and the following evidence indicates that they were juxtaposed as magmas. (1) A well-developed magmatic foliation (using criteria of Paterson et al. (1989) and Vernon (2000)) is common to both units, and is generally sub-parallel to contacts between them at the mesoscale (Fig. 10b). This foliation has been observed cutting contacts at the mesoscale only where one unit pinches out into the other (Fig. 10c). (2) At the map scale, the magmatic foliation in the two units cuts the contact in several places (Fig. 6). (3) The contact is gradational, and locally contains tonalite that appears to be a textural hybrid of the two units. (4) At several localities along the eastern contact, both tonalite units and rocks of intermediate to mafic composition are folded together (Fig. 10d). The lack of solid-state deformation indicates that these folds formed in the magmatic state.

According to Murray (1978), contacts between the northern unit and intermediate to mafic sheets are sharper than those between the central unit and the same sheets. Our observations have confirmed this in a very general way, but all gradations between sharp and very diffuse contacts were seen between the sheets and both tonalite units. As noted by Murray (1978) on the basis of textural contrasts there are several locations where variable-sized bodies of one tonalite type are present in the other. In these locations, as along the main contact between the two tonalite units, both share the same magmatic foliation, even where it cuts across contacts.

In summary, the above evidence indicates juxtaposition of the two discrete tonalite units while they were both magmas. The contact between them is intrusive, but we have found no unequivocal field or microstructural evidence for an order of intrusion. Although Murray (1978) suggested that the northern unit was emplaced around the margins of the central unit, later in this paper we conclude instead that the central unit intruded the northern one.

3.2.2. Contact between central and southern units

The contact between these two units is gradational over a zone averaging up to 300 m in width, defined entirely by the concentration of large plagioclase phenocrysts up to 20 mm long in the southern unit (Murray, 1978). The foliation shared by the two units is magmatic in origin, and is everywhere oblique to the gradational contact (Fig. 6). Murray (1978) noted that the two units may be either textural variants from a single pulse, or two separate pulses that mixed extensively at their margins.

3.3. Structures, microstructures and kinematics

3.3.1. Foliations

A foliation is present throughout most of the pluton (Figs. 4 and 6), and is magmatic in origin on the basis of microstructures (described below) observed in thin sections from 102 samples throughout the pluton (Fig. 3). In the marginal northern unit, this foliation has been overprinted by a solid-state foliation defined mainly by biotite, which has recrystallized into platy aggregates of fine- to medium-grained crystals. The strength of this foliation diminishes rapidly from the wall-rock contact towards the pluton interior. Within 100–200 m of the wall-rock contact in

Fig. 10. (a) Eastern contact zone between the northern and central units. A dike of intermediate composition has intruded the northern unit. The dike has pillowed into the tonalite to form microgranitoid enclaves, indicating that the tonalite was still a magma when the dike intruded. Hammer for scale. (b) Typical contact between the northern and central units. Although difficult to see in the northern unit, magmatic foliation in both units is sub-parallel to the contact. Diameter of lens cap 65 mm. (c) Relatively uncommon contact relationship between the northern and central units in the eastern half of the pluton. The two units are interlayered, and the magmatic foliation shared by both cuts across the contacts with no deflection. Diameter of coin 21 mm. (d) Eastern contact zone between the northern and central units. Both tonalite units and intermediate to mafic units are folded together. There is no evidence for solid-state deformation, indicating that the various rock types were juxtaposed and folded in the magmatic state. Hammer for scale. (e) S–C structures near western margin of pluton. Diameter of coin 21 mm. (f) Solid-state lineation developed in the marginal northern unit, near the northern edge of the pluton. Narrow, dark lenses are aggregates of streaked, recrystallized biotite as seen on the solid-state foliation surface. Diameter of coin 25 mm. (g) Photomicrograph in plane polarized light showing solid-state foliation near the outer margin of the northern unit. Quartz and biotite have recrystallized into monomineralic aggregates separating plagioclase crystals. Hornblende and plagioclase have also undergone minor deformation. Long axis of photomicrograph 40 mm. (h) Photomicrograph in plane polarized light showing S–C structures near the outer edge of the marginal northern unit. Quartz and biotite are strongly recrystallized along the 'C' surfaces. Hornblende and plagioclase are locally deformed, and plagioclase recrystallized, along their margins. Long axis of photomicrograph 21 mm.

these areas, S–C-type structures occur (Fig. 10e); the 'S' surfaces represent the modified initial magmatic foliation, and the 'C' surfaces form discrete lenticular layers 1–3 mm thick and several centimeters long.

The magmatic foliation is generally parallel to schlieren and the long axes of elongate microgranitoid enclaves, but is locally oblique to these features. In general, the magmatic-foliation intensity decreases from north to south in the pluton. Typically the highest enclave aspect ratios occur in the marginal northern unit, where solid state fabrics overprint magmatic fabrics and axial ratios of elongate microgranitoid enclaves reach values up to 20:1. In the northern unit, enclave aspect ratios rapidly diminish to values of $<3:1$ toward the interior of the unit, thus defining a major fabric-intensity gradient. The foliation intensity increases in the northern and central units near their mutual contact, and particularly in the central unit, where microgranitoid enclave ratios are commonly 4:1 to 6:1 and locally reach ratios greater than 10:1. The foliation in both units near their mutual contact is entirely magmatic, and so these fabric-intensity gradients developed during juxtaposition of two magmas. The foliation in the southern unit is generally weak or absent, defined commonly by slightly elongate enclaves (2:1 or less), and its intensity does not change at the gradational contact with the central unit. Except for a weak increase at the far eastern side of the southern unit, the foliation intensity in this unit does not increase systematically towards the wall-rock contacts.

The trend map in Fig. 6 shows that the foliation is strongly concordant to wall-rock contacts in the northern unit, largely concordant to the contact between the northern and central units, and strongly discordant to the contacts between the central and southern units, and between the southern unit and its wall rocks.

3.3.2. Lineations

Lineations are present throughout much of the pluton (Fig. 5) and, as with foliations, they can be divided into magmatic and solid-state varieties. With the exception of those in the marginal northern unit, all lineations are magmatic in origin and are best-defined by preferred alignment of hornblende crystals and elongate enclaves observed on magmatic foliation surfaces. In much of the northern unit, lineations are difficult to find, owing to the equant hornblende shapes, whereas those in the central unit are easier to find, owing to the elongate hornblende shapes. Lineations in the central unit are well-developed near the contact with the northern unit, but were only locally observed within its interior. As with the foliations, lineations are generally weakly developed in the southern unit.

In the marginal northern unit, a solid-state lineation formed in conjunction with the solid-state foliation, and is clearly visible on foliation surfaces, where it is defined mainly by streaks of recrystallized biotite (Fig. 10f). This solid-state lineation is parallel to the long axes of elongate microgranitoid enclaves, suggesting that it overprinted a pre-existing magmatic lineation. As with the foliation, the lineation intensity decreases in the northern unit towards its interior, where enclaves form oblate shapes with no single principal direction of extension. The paucity of lineation data, compared with foliation data (Figs. 4 and 5), in the interior portion of the northern unit reflects this gradient in relative development of the linear component of the magmatic fabric. Magmatic lineations and a single long axis of enclave shapes are more strongly developed near the contact between the northern and central units (Fig. 5).

A sharp change in lineation orientation occurs near the northeastern margin of the pluton, in concert with a change from magmatic to solid-state deformation. Lineations in the magmatic part of the northern unit trend northeast, but deflect sharply to the north within the marginal northern unit (Figs. 5 and 7).

3.3.3. Microstructures

Microstructures in the San José pluton dominantly record magmatic deformation. Magmatic foliations and lineations are marked by alignment of igneous biotite, hornblende and plagioclase. Solid-state deformation fabrics in the pluton are generally restricted to the marginal northern unit. Bending of plagioclase crystals and weak undulose extinction in quartz are present locally throughout the pluton, and particularly along the contact between the northern and central units. However, these microstructures indicate very low strains and could have been caused by melt-present deformation at low volume percentages of melt, combined with volumetric changes associated with cooling and contraction of the pluton.

Evidence for minor fracturing and alteration is also present throughout the pluton. These fractures are locally occupied by white mica, chlorite, and epidote. Although we have found no evidence for regional accumulation of ductile strain after pluton emplacement, several kilometers of oblique, brittle/ductile, contractional displacement apparently occurred on the Rosarito fault (Fig. 2) from ca. 100–85 Ma (Schmidt and Paterson, 2002). We suggest that the late fracturing and alteration in the pluton was probably associated with this faulting.

In the marginal northern unit, a gradient in solid-state fabric intensity occurs from approximately 1 km from the wall-rock contact outward. As the degree of solid-state deformation increases, quartz and biotite are increasingly recrystallized into monomineralic aggregates separating locally recrystallized plagioclase crystals (Fig. 10g). At the highest strains, hornblende deforms by fracturing and plagioclase is more commonly recrystallized, indicating medium- to high-temperature conditions during the solid-state deformation. The overall result is an anastomosing fabric that overprints a pre-existing magmatic one. Even in zones of high solid-state strain, the original magmatic fabric can still be recognized in the form of aligned hornblende and plagioclase crystals.

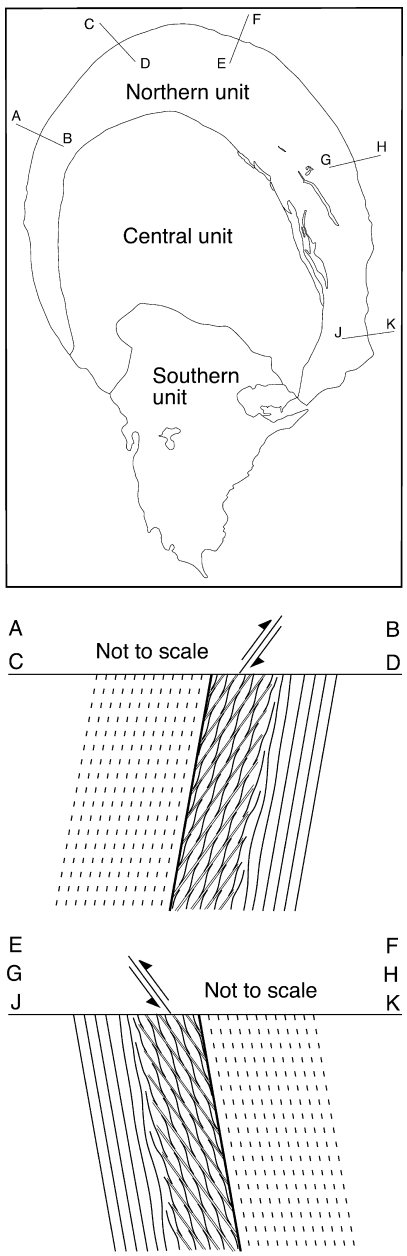

Fig. 11. Generalized cross-section along the lines shown in the map. The sections illustrate that the S–C structures around most of the outer margin of the northern unit indicate wall-rock-over-pluton sense of displacement.

S–C structures are present in the zones of highest strain, near the wall-rock contact (Fig. 10e); their formation involved simultaneous intensification and modification of the pre-existing magmatic foliation, and the development of cross-cutting shear surfaces (Fig. 10h). Quartz and biotite are strongly recrystallized in the 'C' surfaces, and individual aggregates of biotite appear to have been extensively smeared along them to become interconnected. Hornblende is fragmented and plagioclase is recrystallized, indicating medium- to high-temperature conditions during S–C formation.

3.3.4. Kinematics

The S–C structures (Fig. 10e and h) are systematically developed within the marginal northern unit. On the west side of the pluton, they occur only along its northern third. They continue north around the pluton to the area where the lineations converge to down-dip orientations; in this area, the S–C structures are only locally developed. Just east of this area, they pick up again and are present around the entire northeastern two-thirds of the pluton, disappearing where the pluton contact turns sharply from a north–south strike to a northeast–southwest strike. Without exception, these structures indicate a country-rock-side-up sense of displacement (Fig. 11), parallel to the solid-state lineation.

4. Adjacent country rocks

4.1. Rock types

The San José pluton lies entirely within the Late Cretaceous (Aptian–Albian) Alisitos Formation (Allison, 1955, 1964, 1974). Johnson et al. (1999b) separated the Alisitos Formation in Fig. 2 into two principal units. In the southwest, the rocks are dominantly volcaniclastic mudstones, siltstones and sandstones, all apparently deposited in a subaqueous environment. To the east, these rocks are abruptly juxtaposed against a marine volcano-sedimentary basinal assemblage that surrounds the San José pluton. This assemblage contains similar rocks to those in the southwest, but also includes reef limestones (now marble), calc–silicates, pyroclastic deposits and volcanogenic conglomerates.

On the basis of fossil assemblages in these rocks, Allison (1964, 1974) concluded that they were deposited in the Aptian. We have recently collected SHRIMP U/Pb zircon data from these volcanogenic rocks directly northwest of the San José pluton (Fig. 2), near a fossil locality reported by Silver et al. (1963), and our 114.8 ± 1.5 Ma age (see Fig. 2 and geochronology section below) is consistent with Aptian deposition.

Rocks east of the Main Mártir Thrust include calc–silicate, volcaniclastic and sedimentary rocks, tuffs, orthogneisses, sheeted intrusions and deformed K-feldspar-bearing plutons. Many of these rocks show mylonitic microstructures and, unlike the Alisitos Formation, commonly show evidence for multiple deformations. The intrusive rocks range in age from Middle Jurassic (Schmidt and Paterson, 2002) to Early Cretaceous (Fig. 2); thus, an older component of intrusive rocks form country rocks for younger Cretaceous intrusions, such as the nearby Cerro de Costilla complex and the Sierra San Pedro Mártir pluton.

4.2. Metamorphism

Rocks of the Alisitos Formation shown in Fig. 2 mostly underwent lower greenschist-facies regional metamorphism, but a gradient to upper greenschist-facies or lower amphibolite-facies occurs to the east, adjacent to the Main Mártir Thrust. Garnet–biotite assemblages occur in appropriate rock types within 200–300 m west of the Main Mártir Thrust along most of its length in Fig. 2. With the exception of younger, post-thrust Cretaceous intrusions, rocks east of the thrust have been metamorphosed at upper amphibolite-facies conditions, with abundant migmatite.

The San José pluton is surrounded by a hornblende hornfels-facies contact metamorphic aureole. Although slight recrystallization effects related to the pluton extend ca. 1 km from its margins, hornblende hornfels-facies metamorphic mineral assemblages are generally restricted to within 400 m of the contact (Murray, 1978). The rocks north and northeast of the pluton all appear to show the effects of contact metamorphism from both the San José pluton and the Cerro de Costilla complex. Andalusite has been found sporadically in these aureole rocks, consistent with the relatively low emplacement pressures (ca. 2.6 kbar) obtained for the Zarza Intrusive Complex to the southwest (Johnson et al., 1999a).

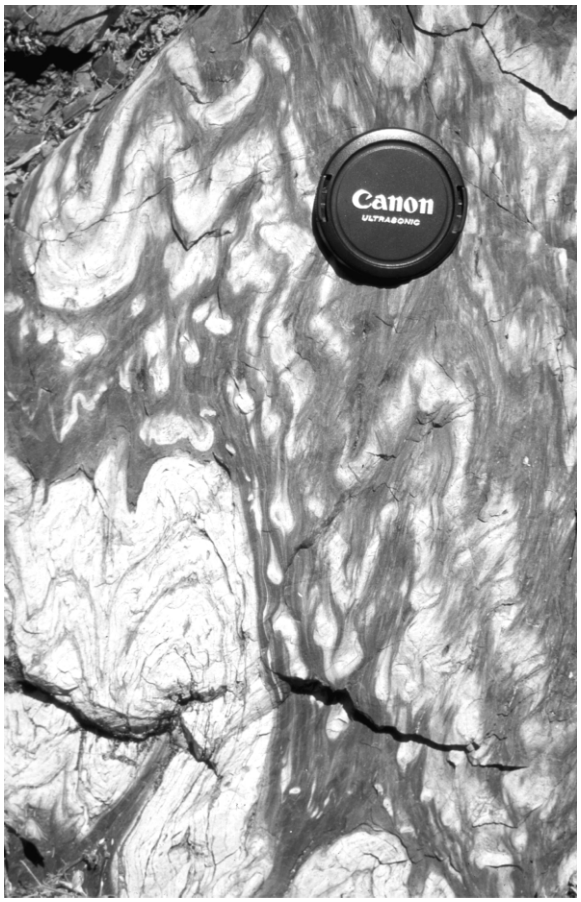

Fig. 12. Tightly folded calc–silicate rock of the Alisitos Formation approximately 3 km south-southeast of the San José pluton, 1.5 km north of the Potrero pluton. Diameter of lens cap 65 mm.

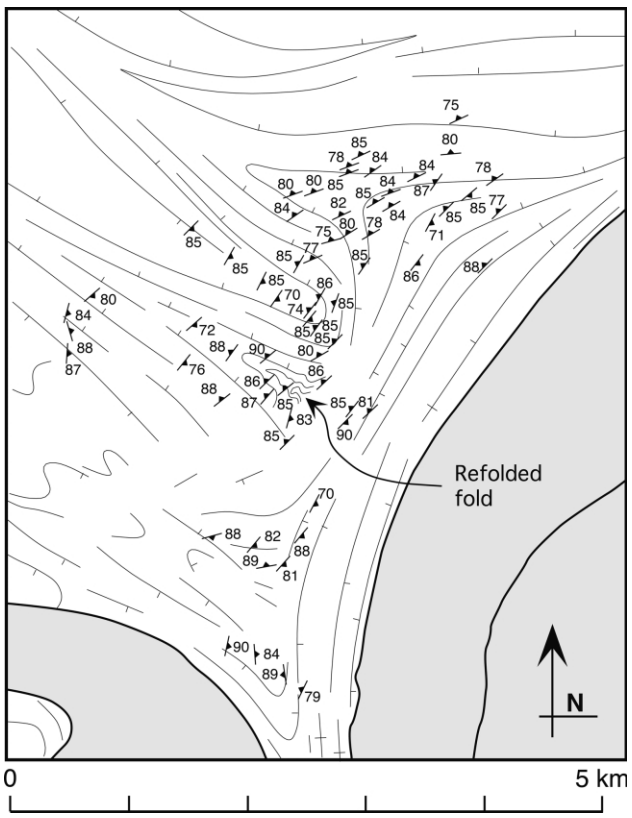

Fig. 13. Map of the northwestern triple point of the pluton showing emplacement-related foliation that cross-cuts all regional structures, and the trend-lines and dip directions for bedding/compositional layering. The map shows only those measurements where the foliation is oblique to bedding/compositional layering. Closer to the pluton, this foliation is parallel to the compositional layering, which is transposed parallel to the pluton margin. Note that the emplacement-related foliation forms the axial surface to refolds of tight to isoclinal regional folds. This emplacement-related foliation is the latest structure observed in the triple point region, indicating that emplacement occurred after, or very late during the waning stages of, the regional deformation.

4.3. Structures, microstructures and kinematics

4.3.1. Folds and foliations

A marked regional deformation gradient occurs in the Alisitos Formation, with deformation intensity increasing from west to east towards the Main Mártir Thrust (Johnson et al., 1999b). In the southwest, near the Zarza Intrusive Complex (Fig. 2), folds are open to close and upright, with poorly to moderately developed axial-surface foliations. Directly southwest of the San José pluton, the folds shown in Fig. 6 are close to tight, upright to gently plunging, with a well developed axial-surface foliation in most rock types. In the areas northwest and east of the San José pluton (Fig. 6), folds become tight to isoclinal (Fig. 12), overturned to the southwest, and moderately plunging to reclined (down-dip axes). They remain this way east to the Main Mártir Thrust,

where they are juxtaposed against older rocks with a more complex deformation history.

A strong ductile deformation aureole is present around most of the pluton. In the northwest, where regional bedding and foliation trends are highly oblique to the pluton margin, a distinct margin-parallel foliation cuts them both as far as 3 km from the pluton (Fig. 13). At the outer reaches of its occurrence, the foliation appears as a very fine, faint crenulation cleavage, and its intensity increases progressively towards the pluton. Near the pluton margin, where this foliation is pervasive and regional bedding and foliations have been isoclinally folded and transposed parallel to the margin, deformed clasts commonly have axial ratios up to 15:5:1 (Murray, 1978 and our own observations). This contact-parallel foliation remains strong around the entire northern two-thirds of the pluton, but is strongest around the northern third.

In contrast, a strong margin-parallel foliation is absent around the southwestern quarter and southern tip of the pluton. In these locations bedding, foliations and folds are sharply truncated by the pluton, and the rocks have been pervasively fractured along several prominent joint sets. Stoping was an important process in these areas, as evidenced by abundant stoped blocks, some larger than 100 m across. Axial ratios of deformed clasts in these rocks rarely exceed 4:1 in two-dimensional sections (Murray, 1978 and our own observations). However, a clear deformation gradient occurs as the pluton is approached from the southwest, and regional folds are overturned adjacent to the pluton (Fig. 6).

Within the deformation aureole, the regional folds northwest of the pluton are locally refolded about axial surfaces parallel to the pluton margin and perpendicular to the regional folds (Fig. 13). Combined with the sharply truncated regional folds along the southern and southwestern pluton margins, they indicate that emplacement largely post-dated the regional folding.

4.3.2. Lineations

A regional intersection lineation is well-developed in the Alisitos Formation away from the pluton, and is particularly clear in the northwest of Fig. 5, where its regional, down-dip orientation is relatively undisturbed by intrusions. The orientation of this lineation changes progressively as the pluton is approached from the northwest. Within the deformation aureole around the pluton, a lineation is parallel to the long dimensions of deformed clasts and marks the direction of maximum finite elongation. Because only one lineation has generally been observed in any one outcrop, and given the progressive changes from regional orientations to those adjacent to the pluton, we suggest that the regional intersection lineation has been progressively rotated into the stretching direction in the deformation aureole.

To analyze the progressive changes in lineation orientation around the pluton, we selected three subareas for evaluation. Fig. 14 shows the lineations around the northern part of the pluton and a series of equal-area projections that illustrate the progressive change in orientations as the pluton is approached from the northwest, north and northeast. The first net shows 19 measurements of the regional intersection lineation well away from the pluton to the northwest, and the solid black dot represents the mean of these data; this mean orientation is plotted on the other projections. In the northwest (subarea A), the data indicate a progressive rotation from the regional orientation to the shallower northeast-plunging orientations in the deformation aureole around the pluton. Directly north of the pluton (subarea B), the data indicate a progressive rotation from the regional orientation to: (a) the steeper plunges adjacent to the northern pluton contact, and (b) the shallower northeast- and northwest-plunging orientations adjacent to the northwestern and northeastern margins of the pluton, respectively. In the northeast (subarea C), the situation is different. Lineations adjacent to the contact cluster around the regional orientation, with shallower northwest-plunging lineations occurring further out in the country rocks. See the caption to Fig. 14 for further discussion.

Owing to the late emplacement timing of the pluton relative to the regionally-developed structures, these systematic changes in lineation orientation were probably caused largely or entirely by emplacement, rather than later regional deformation; thus, they will be used below to constrain our interpretation of emplacement kinematics.

4.3.3. Microstructures

Microstructures present in the contact metamorphic aureole indicate that deformation was synchronous with the prograde contact metamorphism. For example, calc–silicate rocks adjacent to the pluton on its northwestern side contain garnet, clinopyroxene and hornblende that have been strongly deformed and recrystallized. No appreciable evidence was found for low-temperature deformation after emplacement-related deformation and metamorphism.

4.3.4. Kinematics

In constrast to the S–C surfaces in the pluton margin around much of its northern two-thirds, kinematic indicators in the adjacent wall rocks are rare. Three locations have been found adjacent to the pluton margin, in which sense of shear can be unambiguously determined; two of these show pluton-side-up, and the other shows pluton-side-down. Apart from these isolated examples, wall-rock fabrics adjacent to the pluton are very symmetrical, but the well-developed, moderately- to steeply-plunging elongation lineation indicates that material in the aureole stretched out of the map-view section during emplacement.

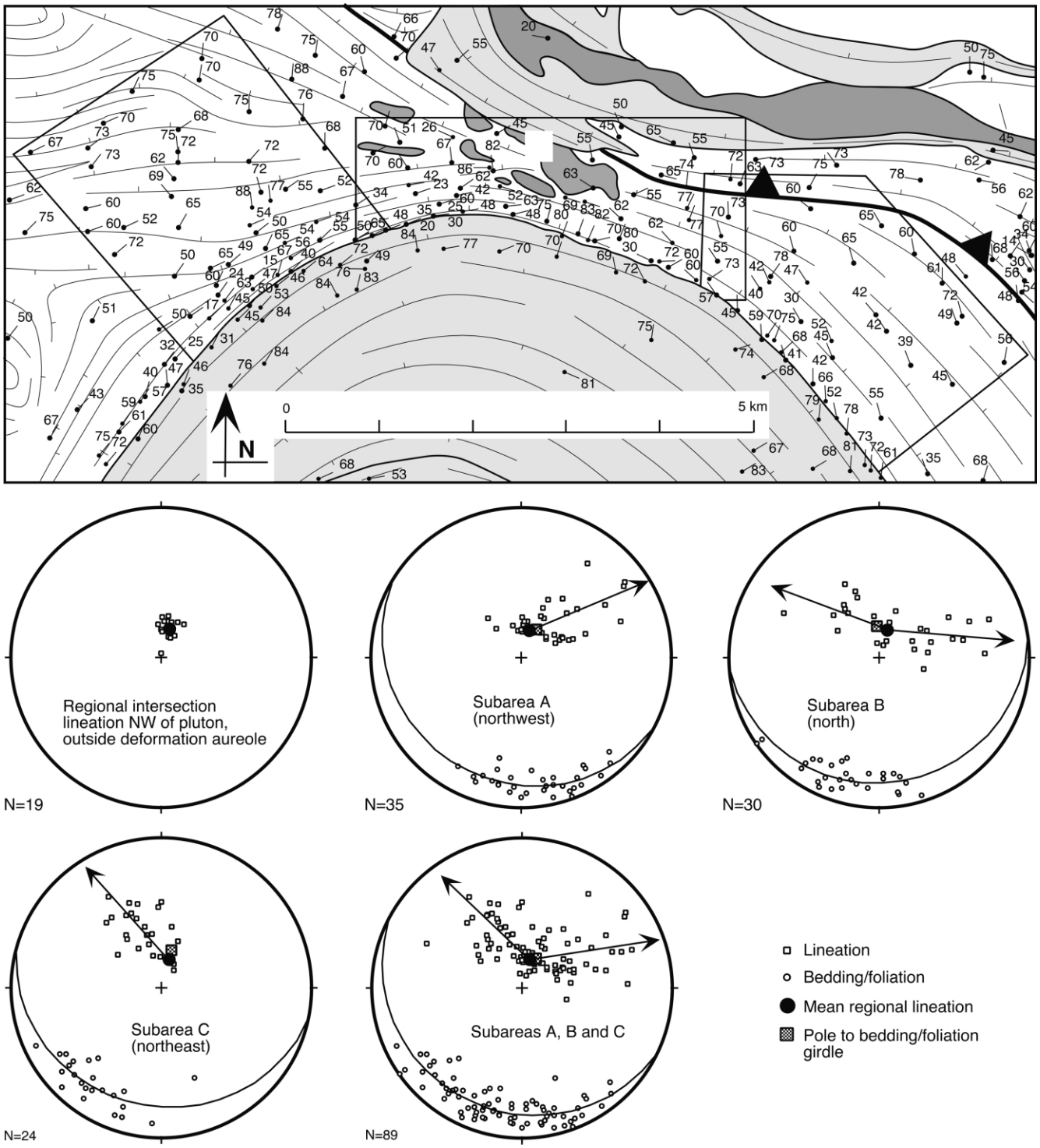

Fig. 14. Map of the northern portion of the pluton showing lineation data. The data from three subarea—A, B and C—are shown in the equal area diagrams. In addition, the upper-left equal area diagram shows the regional intersection lineation well away from the pluton to the northwest. The mean orientation of this regional lineation is plotted in all the other equal area diagrams as filled black circles, and the arrows are shown emanating from them. The equal area plots indicate the following. In subareas A and B, the regional intersection lineation has been rotated into parallelism with the direction of maximum finite elongation adjacent to the pluton. In subarea C, lineations adjacent to the pluton contact cluster around the mean regional lineation orientation, whereas shallower northwest-plunging orientations occur away from the contact. As shown in the summary, equal area diagram at bottom-center, poles to bedding/foliation in the wall rocks fall along a great circle, indicating that the originally steeply-dipping bedding/foliation has simply been folded around the steeply-dipping pluton margin. In addition, the pole to this great circle is approximately parallel to the mean regional lineation orientation. This requires that the variation in lineation orientations in subareas A, B and C is not due to folding of the compositional layering around this pole, supporting the idea that the regional lineation has been rotated into the stretching direction adjacent to the pluton.

5. SHRIMP U–Pb geochronology

5.1. Procedures

A heavy mineral concentrate, generally highly enriched in zircon, was prepared using standard crushing and separating procedures. Zircon grains were hand picked from the mineral separate, mounted in epoxy together with chips of the AS3 and SL13 reference zircon, sectioned approximately in half and polished. Reflected and transmitted light photomicrographs and cathodoluminescence (CL) SEM images were prepared for all zircon grains. The CL images were used to decipher the internal structures of the sectioned grains and to target specific areas within them for analysis.

The U–Th–Pb analyses were made using SHRIMP II at the Research School of Earth Sciences, The Australian National University, Australia, following standard procedures as given by Williams (1998) and references therein. Each analysis consisted of six scans through the mass range. The data have been processed using the SQUID Excel Macro ofLudwig (2000). The Pb/U ratios have been normalized relative to a value of 0.1859 for the $^{206}Pb/^{238}U$ ratio of the AS3 reference zircon, equivalent to an age of 1099 Ma (Paces and Miller, 1993). Uncertainties given for individual analyses (ratios and ages) are at the one σ level; however, the uncertainties in calculated weighted mean ages are reported as 95% confidence limits. The Tera and Wasserburg (1972) concordia plots, relative probability plots with stacked histogram, and weighted mean $^{206}Pb/^{238}U$ age calculations have been made using ISOPLOT/EX (Ludwig, 1999).

5.2. Results

Five new SHRIMP U–Pb ages are reported here; three from the San José pluton, one from the surrounding Alisitos Formation directly northwest of the San José pluton, and one from the Sierra San Pedro Mártir pluton (see Fig. 2). The data tables for all analyses can be accessed at the Journal of Structural Geology Electronic Annex, or from the principal author. Because we are concerned here primarily with the temporal evolution of the San José pluton, we have also lodged the concordia plots, relative probability plots and stacked histograms, and discussion for the other two samples in the electronic annex.

5.2.1. San José pluton samples

Data for each of the three units of the pluton were collected in two stages, from different grain mounts (Table 1, electronic annex). Initially, we collected the data reported in Johnson et al. (1999b). In order to make more direct comparisons among the three units, a second mount was prepared, so that all three units could be analyzed in a single SHRIMP analytical session (mount Z3617, Table 1). A notable feature of zircon from the three units is the dominant, uniformly low U content. Therefore, at ca. 100 Ma, the amount of radiogenic Pb is very low, giving rise to higher relative proportions of common Pb (ca. 2–10% ^{206}Pb common) and higher analytical uncertainties in the radiogenic ratios and calculated ages (ca. 2–3% for an individual analysis at 1-σ level).

5.2.1.1. Northern unit. Zircon from this sample is notably very coarse grained, many crystals being greater than 400 μm in length (Fig. 15a). The grains are clear and, whereas the smaller grains tend to have pyramidal terminations, the larger grains are elongate and appear to be fragments of grains that may have originally had pyramidal terminations (prior to crushing and separation). The CL images show a dominantly simple, zoned magmatic internal structure; some grains are sector zoned.

Twenty-three analyses on 20 grains were made on mount Z3060 and 24 grains were analyzed on mount Z3617. The analyses of grains 20 and 23 on mount Z3617 did not yield data, due to an unusual and rare machine malfunction. Preliminary data assessment for mount Z3060 yielded an age of 108 ± 1.0 Ma, as reported by Johnson et al. (1999b). The total data set has been reprocessed (Table 1) using SQUID (Ludwig, 2000).

The generally low U content and low radiogenic Pb are highlighted on the Tera–Wasserburg concordia plot (Fig. 15b), in which the analyses show significant enrichment in common Pb. The radiogenic ages show some dispersion on the relative probability plot (Fig. 15b), and a weighted mean of the $^{206}Pb/^{238}U$ ages for all 45 analyses gives 105.6 ± 1.2 Ma (MSWD = 1.7). The relative probability curve appears to be skewed, with a longer tail on the younger age side. Four analyses from the Z3617 mount yield slightly younger ages, namely analysis 5.1 and 6.1 at ca. 97 Ma, and analyses 14.1 and 18.1 at ca. 95.5 Ma. Correspondingly, three analyses from mount Z3060 may be slightly older, namely analysis 6.1 at ca. 111 Ma, and 6.2 and 11.1 at ca. 112 Ma. Exclusion of these seven analyses does not significantly alter the weighted mean $^{206}Pb/^{238}U$ age, giving 105.8 ± 1.1 Ma (MSWD = 1.07). The best estimate for the crystallization age of the large, simple, zoned magmatic zircon in this sample is therefore 105.6 Ma ± 1.2 Ma.

5.2.1.2. Central unit. Zircon crystals from this sample are clear and elongate, with bipyramidal terminations (Fig. 15c). They are mostly ≤200 μm in length. Some more equant, squat grains also have pyramidal terminations. The CL images show a simple, zoned, magmatic internal structure; some grains are sector zoned, whereas others have truncated magmatic zoning that may reflect different stages of magmatic zircon growth.

Seventeen effective analyses were made on mount Z3427, and 24 analyses on 21 grains were analyzed on mount Z3617. The analysis of grain 20 on mount Z3617 is

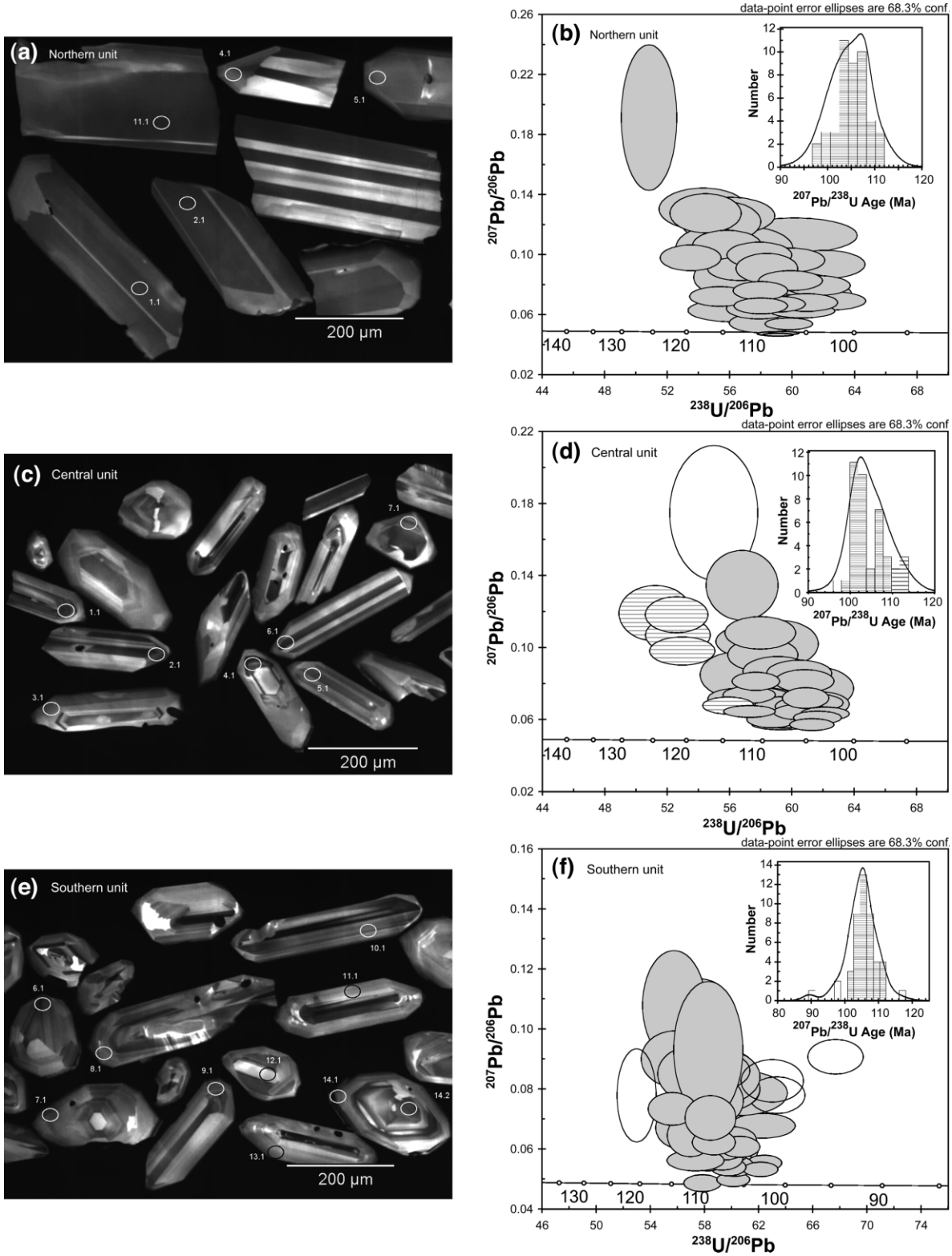

Fig. 15. Cathodoluminescence SEM images ((a), (c) and (e)) of zircon grains, and Tera–Wasserburg concordia plots and relative probability plots ((b), (d) and (f)), for the northern, central and southern units of the San José pluton. White numbers and ellipses in the SEM images indicate analysis points. All data tables, and additional information for samples from the Alisitos Formation and Sierra San Pedro Mártir pluton, can be found in the electronic annex. See text for discussion.

significantly enriched in common Pb, is considered to be inferior, and so it is not included in the data table. The session on mount Z3427 was severely interrupted by machine problems and although 25 analyses were attempted on 20 grains, only 17 yielded data. Preliminary data assessment for mount Z3427 yielded an age of 104.8 ± 1.8 Ma, as reported by Johnson et al. (1999b). The total data set has been reprocessed using SQUID (Ludwig, 2000) as given in Table 1.

On the Tera–Wasserburg concordia plot (Fig. 15d), five analyses lie significantly to the higher-age side of the main grouping (analyses 14.1, 16.1, 17.1 and 17.2 from Z3427, and analysis 11.2 from Z3617, with $^{206}Pb/^{238}U$ ages of ca. 111–114 Ma). The relative probability plot (Fig. 15d) further highlights these older analyses, and a general skewing of the probability peak towards older ages. The structural discordance of zoned central regions to zoned rim regions may represent a real crystallization age difference. However, the low U content leads to low radiogenic Pb and high uncertainties in the calibrated U/Pb ratios.

If these five older analyses, and one younger analysis (11.1 from mount Z3427) are excluded, a weighted mean of the remaining 35 gives 103.4 ± 1.0 Ma (MSWD = 1.11), which we consider to be the best estimate for the magmatic crystallization of simple, zoned zircon in this sample.

5.2.1.3. Southern unit. Zircon crystals from this sample are clear and elongate, mostly with bipyramidal terminations (Fig. 15e). The grains are ca. 200 μm in length, though some more equant, squat grains are ca. 100 μm or less in diameter. The CL images show a simple, zoned, magmatic internal structure; some grains are sector zoned, whereas others have truncated zoning that may reflect different stages of magmatic zircon growth.

Twenty-three analyses on 20 grains were made on mount Z3060 and 24 analyses on 23 grains were made on mount Z3617. The analysis of grain 22 on mount Z3617 did not yield data, owing to an unusual and rare machine malfunction. Preliminary data assessment for mount Z3060 yielded an age of 106.7 ± 1.2 Ma as reported inJohnson et al (1999b). The total data set has been reprocessed herein (Table 1) using SQUID (Ludwig, 2000).

The areas analyzed in mount Z3060 tend to be higher in U, and therefore radiogenic Pb, with lower common Pb than those in Z3617. Some scatter in $^{238}U/^{206}Pb$ ratios, as seen in the Tera–Wasserburg concordia plot (Fig. 15f), is in part due to the better constrained U/Pb ratios (relative to the northern unit above). However, on a relative probability plot, with stacked histogram (Fig. 15f), this scatter is clearly caused by three relatively young analyses (6.1, 14.1 and 17.1 from Z3617, Table 1) and one significantly older analysis (20.1 from Z3617, Table 1). No features distinguish these four areas from others in the transmitted or reflected light photomicrographs, nor the CL images. The younger analyses at ca. 89 and ca. 97 Ma are interpreted to be of areas that have lost radiogenic Pb, whereas the older analysis of grain 20 at ca. 116 Ma may reflect inheritance of zoned magmatic zircon from the surrounding Alisitos Formation (see sample SJ430A, Electronic Annex, and age of 114.8 ± 1.5 Ma in Fig. 2).

A weighted mean of all 46 analyses has excess scatter at ca. 105 Ma (MSWD = 3.8). If the four analyses noted above are excluded, the weighted mean $^{206}Pb/^{238}U$ age is 105.4 ± 1.1 Ma (MSWD = 1.6), which is the best estimate for the crystallization age of the simple, zoned magmatic zircon in this sample.

5.2.1.4. Summary. The SHRIMP U–Pb ages for the three pluton samples cannot be separated within the uncertainty limits, primarily owing to the low U content of the zircon. The field evidence suggests that the central unit intruded the northern unit, and the SHRIMP data are consistent with this interpretation. In addition, the markedly different zircon populations in the two units (Fig. 15a and c) support two separate pulses of magma. The temporal relationship between the central and southern units remains less clear, and will be discussed further below.

6. Critical evidence for the emplacement history

6.1. Introduction

Several observations around and within the San José pluton provide unusually good constraints on the emplacement history, and these are summarized below. Most of these observations are consistent with a component of lateral expansion in association with either diapirism or dike-fed expansion.

6.2. Late emplacement timing relative to regional deformation

The pluton appears to have been emplaced very late in the regional deformation history, because: (1) tight regional folds, bedding and regional foliation are sharply truncated along the southwestern margin of the pluton (Fig. 6); (2) displacement vectors for S–C surfaces in the marginal northern unit are approximately parallel to the solid-state lineation in the pluton and wall rocks adjacent to the pluton margin, consistent with northward pluton expansion; (3) no evidence has been found at any scale for deformation fabrics overprinting the contact-parallel foliation in the pluton or wall rocks where they lie at a high angle to the NE–SW regional shortening direction; (4) SHRIMP U/Pb zircon data identify the pluton as part of a ‘stitching’ phase of magmatism that occurred after crustal thickening associated with juxtaposition of the western and eastern part of the batholith (Johnson et al., 1999a,b); (5) isoclinal regional folds are refolded about axial surfaces parallel to the pluton margin in the northwestern triple point (Fig. 13); and (6) the contact-parallel foliation in wall rocks of the northwestern

triple point overprints all regional deformation fabrics (Fig. 13). As noted by Brun and Pons (1981), Bateman (1984), and Lagarde et al. (1990), the presence of such a foliation overprinting all regional structures is consistent with emplacement postdating, or occurring very late during, regional deformation. No unequivocal evidence has been found for appreciable post-emplacement regional ductile deformation within or around the pluton, so structures observed within the pluton and its deformation aureole appear to be largely or entirely the result of pre-emplacement and emplacement-related deformation.

6.3. Kinematics in the outer solid-state margin of the pluton

S–C structures in the marginal northern unit of the pluton invariably indicate wall-rock-up movement. Importantly, they are present only where the pluton contact dips outward (northern and eastern contacts); so they indicate wall-rock over pluton displacement (Fig. 11). This displacement is compatible with asymmetrical pluton expansion, at least relatively late in the emplacement history. A general lack of appreciable solid-state deformation in the main body of the pluton indicates that expansion occurred while the bulk of the pluton still contained a substantial percentage of melt. Wall-rock-up sense of shear is also consistent with sinking of the pluton after crystallization (e.g. Glazner, 1994; Weinberg and Podladchikov, 1995; Glazner and Miller, 1998; Johnson et al., 1999a). Although this remains a possible explanation for the S–C structures, we have difficulty understanding why they would only form where the contact is dipping outward, and why their displacement vectors would in general be oriented parallel to the solid-state lineations, rather than down the dip.

6.4. Rotated lineations in country rocks

If regional intersection lineations have rotated into parallelism with the direction of maximum finite elongation adjacent to the pluton, as the data suggest (Fig. 14), then these rotations could not have been caused solely by vertical movement of the pluton. The lineations adjacent to the pluton all plunge moderately to steeply northward, converging on an area near the pluton's northern margin, where they plunge down the dip. This pattern is consistent with deflection of initially down-dip lineations around an *outward-dipping* body (at the present level of exposure) expanding laterally northward (Fig. 14), and thus suggests a lateral component of pluton growth during emplacement.

6.5. Southward country-rock deflection prior to stoping

Stoping was an important late-operating mechanism in the southern portion of the pluton. However, the bedding/-foliation trend map (Fig. 6) suggests that, prior to stoping, a strong deflection of bedding and regional foliations occurred around the southern end of the pluton. This indicates that, although country-rock deflections were much more pronounced around the northern half of the pluton, the deflection may have been more symmetrical in the earlier stages of emplacement than the current map pattern suggests.

6.6. Internal pluton contact relations

All observations along the pluton's internal contacts indicate that the different textural units, as well as rocks of intermediate to mafic composition located along the contacts, were juxtaposed as magmas. Of particular importance is the contact between the northern and central units, because relationships there are consistent with the central unit having intruded the northern unit. Murray (1978) favored a model whereby the central unit was emplaced first, and the northern unit was emplaced in a crescent shape along its outer margin. Although we cannot unequivocally rule out this possibility, we argue that the field, microstructural and geochronological evidence favors the northern unit being intruded by the central unit.

7. Proposed intrusive/emplacement history for the San José pluton

We propose a four-stage sequential intrusive history for the San José pluton that involved three distinct, south-migrating episodes of forceful tonalite intrusion, followed by an episode of stoping (Fig. 16).

7.1. Stage 1 (Fig. 16a)

The pluton was initiated by emplacement of the northern unit. We found no unequivocal evidence of how this body ascended and was initially emplaced.

7.2. Stage 2 (Fig. 16b)

After the northern unit had been emplaced, but before it had fully solidified, it was intruded by a nested, off-center pulse of the central unit. During this stage, the pre-existing northern unit may have been forced to expand northward, rotating regional intersection lineations in the wall rocks. We also suggest that the S–C fabrics in the marginal northern unit were formed at this stage, indicating that the thin carapace was largely crystallized. Microstructures preserved in these rocks indicate that some melt was present

Fig. 16. Sequential intrusive history for the San José pluton. See text for discussion. Question marks in (c) indicate that we are uncertain as to how and when the structural domes and basins south of the pluton were formed.

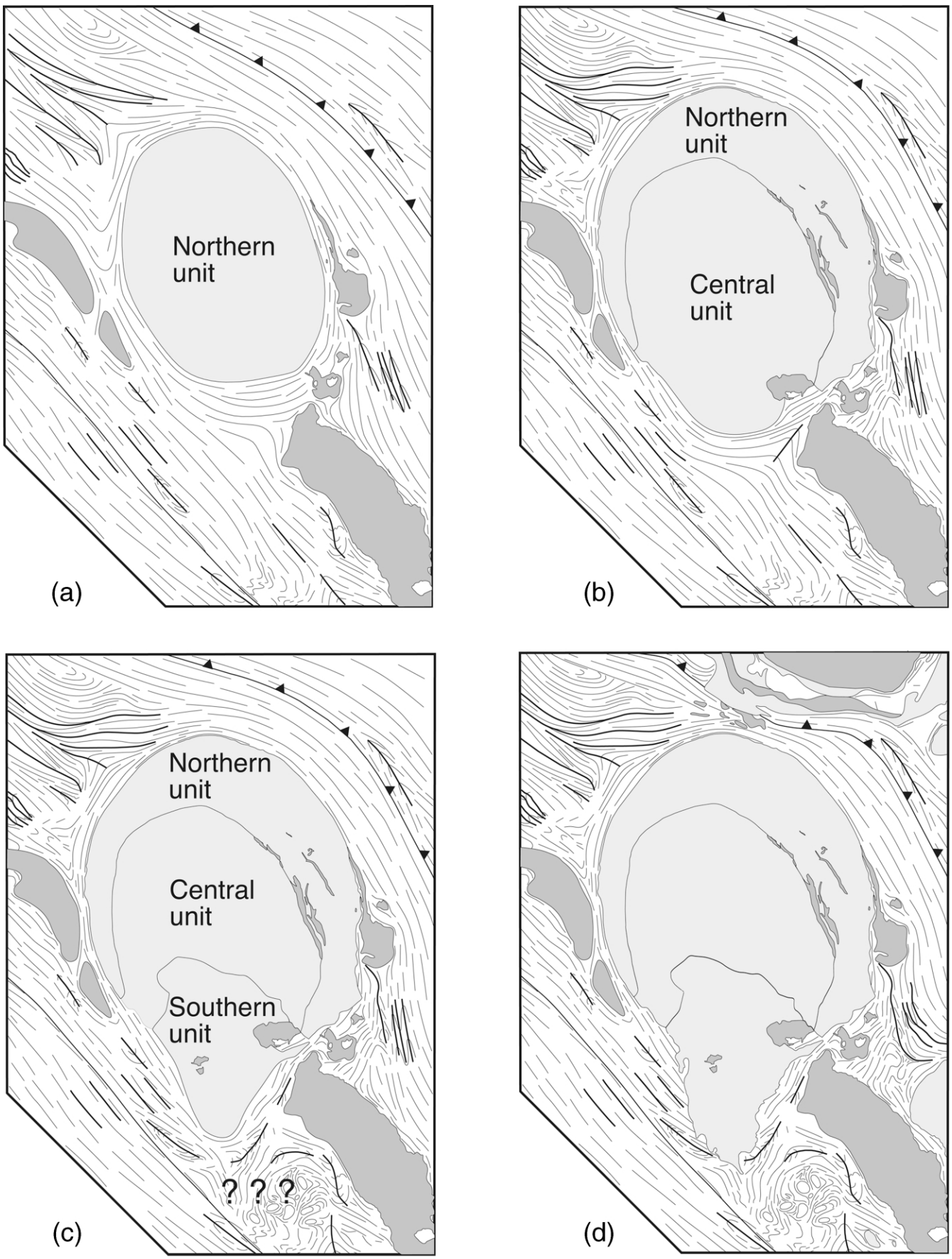
Northern unit
(a)
Northern unit
Central unit
(b)
Northern unit
Central unit
Southern unit
? ? ?
(c)
(d)

during the solid-state deformation. The lack of solid-state deformation in the remainder of the northern unit, combined with the intimate mingling and other magmatic relationships at the contact of the two tonalites, indicate that they were juxtaposed as magmas. Foliations and transposed bedding adjacent to the contact are approximately parallel to the contact throughout most of the northern two-thirds of the pluton, indicating that a high degree of mechanical coupling occurred between the pluton and host rocks during this stage (and probably during Stage 1).

7.3. Stage 3 (Fig. 16c)

After the central unit had been largely emplaced, but before it had solidified, it was intruded by a nested, off-center pulse of the southern unit. As noted by Murray (1978), the southern unit may be a textural variant of the central unit. The southern unit expanded into the still partially molten central unit, but whether or not minor, additional northward expansion of the northern and central units occurred at this stage is unclear. We found no unequivocal field or geochronological evidence for an order of intrusion between the central and southern units. However, the southern unit stoped its surrounding wall rocks (Stage 4 below), and has the weakest foliation and lineation of the three textural units; thus, we favor it as the last of the three to be emplaced.

7.4. Stage 4 (Fig. 16d)

The final act of emplacement was stoping along the southern margin of the pluton. Country-rock trends around the southern margin (Fig. 6) suggest that, prior to stoping, bedding and regional folds and foliations had been deflected southward during emplacement of the southern unit (Stage 3 above); thus, emplacement mechanisms in this part of the pluton evolved through time. The possibility of removing parts of a previously developed ductile deformation aureole around a pluton by late stoping has been emphasized by Paterson and Fowler (1993) and Paterson and Vernon (1995), and the relationships around the southern end of the San José pluton provide evidence of this process.

8. Discussion

8.1. Component of asymmetrical expansion after initial emplacement

Apart from the San José pluton (Murray, 1978, 1979, this study), numerous studies have argued for asymmetrical expansion or inflation of a magma chamber after reaching its emplacement site, for example the Birch Creek pluton (Nelson and Sylvester, 1971), the Papoose Flat pluton (Sylvester et al., 1978; Morgan et al., 1998), the Ardara pluton (Holder, 1979; Siegesmund and Becker, 2000), the Cannibal Creek pluton (Bateman, 1985), the Criffel pluton (Phillips, 1956; Courrioux, 1987), the Chindamora pluton (Ramsay, 1989), and the Flamanville Granite (Brun et al., 1990). Mechanisms for ascent and initial emplacement of these plutons include dikes (Bateman, 1985; Brun et al., 1990), 'wall diapirs' (Sylvester et al., 1978), oblique sills (Morgan et al., 1998), migration along faults (Nelson and Sylvester, 1971), diapirs (Courrioux, 1987) and 'early-stage' diapirs (e.g. Holder, 1979; Ramsay, 1989).

Asymmetrical (non-concentric) expansion has previously been related to rheological variations in surrounding country rocks (e.g. Brun et al., 1990), or to premature crystallization of portions of the pluton margin owing to juxtaposition against carbonates (e.g. Nelson and Sylvester, 1971). The direction of greatest lateral expansion of the San José pluton was north-northeast (Fig. 16; Murray, 1978). Possibly less than 1 Ma before intrusion of the northern unit, high-grade metamorphic rocks to the east-northeast were juxtaposed against the Alisitos Formation along the Main Mártir Thrust (Fig. 2). The presence of relatively hot, partly quartzofeldspathic and pelitic metamorphic rocks to the east of the San José pluton may have been a controlling factor in the preferred direction of lateral expansion. This is particularly compelling when the alternative is considered: westward expansion into Alisitos rocks of dacite to andesite bulk composition (Gastil et al., 1975) and temperatures corresponding to lower greenschist-facies metamorphic conditions. Thus, this study suggests that thermal, compositional and resulting rheological gradients in rocks intruded by plutons may play an important role in controlling directions of pluton expansion.

8.2. Solid-state carapaces around apparently expanded plutons: magma-chamber pressure or post-emplacement deformation?

An important component of in-situ expansion models is how they explain concentric, solid-state foliations in pluton margins. Most previous workers have suggested that pluton margins crystallize at some stage during emplacement, and that continued addition of magma from below causes the plutons to expand. This expansion leads to stretching and ductile deformation of the solid pluton margin, as well as the adjacent wall rocks. This model implies that magmatic pressure in plutons can reach high enough values to deform both the solidified margin and surrounding country rocks. Paterson and Vernon (1995) noted that most plutons inferred by previous workers as having expanded show evidence for post-emplacement deformation, which they suggested may have caused the margin-parallel, solid-state foliations in these plutons (see also Paterson, 1988; Paterson et al., 1991; Vernon and Paterson, 1993). However, the San José pluton differs from many apparently expanded plutons in that: (1) we have found no evidence for post-emplacement ductile deformation in or directly adjacent to the pluton, though the possibility cannot be eliminated; and (2)

there is no evidence for appreciable crystal-plastic strain in the main body, away from the external margins. Thus, the San José pluton is a good candidate for evaluating whether pluton margins can deform in the solid state in response to pluton expansion, without the addition of post-emplacement regional deformation.

8.3. Pluton emplacement mechanisms?

In Section 1 of this paper, we listed a number of emplacement mechanisms commonly invoked for plutons with some or all of the characteristics of the San José pluton. Here, we briefly assess these mechanisms in light of our findings. (1) On the basis of our data and observations, we cannot rule out nested diapirs. (2) Although we cannot rule out downward flow of aureole rocks around the pluton, the downfolding of bedding near a pluton margin that is commonly cited as evidence for this process is not present around the pluton. Nevertheless, the moderately- to steeply-plunging elongation lineation in the deformation aureole of the pluton indicates that ductile aureole flow during emplacement was largely out of the plane of the map section. (3) Although we conclude that a component of lateral pluton expansion accompanied emplacement, we cannot determine whether this was associated with nested diapirs or dike-fed growth. Based on published values for the minimum flow rates and critical widths of granitoid dikes, Johnson et al. (2001) concluded that dike-fed pluton growth should lead to wall-rock strain rates several orders of magnitude faster than those expected around magmatic diapers. We are currently conducting detailed microstructural investigations in and around the San José pluton in search of evidence for high strain rates. (4) On the basis of our data and observations, we conclude that the carapace of solid-state deformation in the northern unit formed largely or entirely during emplacement, as opposed to being formed by post-emplacement regional deformation. (5) We can find no compelling evidence for 'sinking' of the crystallized pluton through its wall and floor rocks. (6) Finally, we find it hard to imagine how floor depression can lead to outward-dipping pluton contacts over 400 m of topographic relief, and a 3-km-wide deformation aureole marked by high strains, strong lateral wall-rock deflections, steep outward dips and the pattern of lineation rotation shown in Fig. 14.

9. Summary and conclusions

The San José pluton contains intrusive, geometric and kinematic evidence consistent with two or three pulses of tonalite, and a component of asymmetrical lateral expansion at the emplacement site. SHRIMP U–Pb zircon data indicate that the entire pluton was constructed in less than 4.4 Ma. Structural data collected within and around the pluton, evidence for lateral expansion, and ductile flow in the deformation aureole are all compatible with nested diapirs or nested dike-fed pulses. One way of possibly distinguishing between these histories is to evaluate the carapace of solid-state deformation, as well as the adjacent wall rocks, for evidence of the very high strain rates that should accompany dike-fed growth (e.g. Johnson et al., 2001); we are currently conducting this work.

The carapace of solid-state deformation occurs along the northern two-thirds of the pluton's outer margin. On the basis of solid-state lineation patterns, and lack of evidence for post-emplacement regional ductile deformation within and around the pluton, we conclude that most or all of this solid-state deformation occurred when the central unit intruded the northern unit, causing a component of lateral expansion in its outer carapace. Shear-sense indicators in the carapace suggest northward expansion, consistent with large wall-rock deflections around the northern end of the pluton. However, moderately- to steeply-plunging elongation lineations in the carapace and adjacent aureole rocks indicate extensive material transport out of the plane of the map section. This study suggests that thermal, compositional and resulting rheological gradients in rocks intruded by plutons may play important roles in controlling directions of pluton expansion.

The well-preserved transition from magmatic flow to solid-state deformation in the margin of this pluton provides a rare opportunity to study fabric evolution related to pluton emplacement, and we are currently pursuing this research.

Acknowledgements

This work was supported by National Science Foundation Grant EAR 0087661 (SEJ), Australian Research Council Large Grant A39700451 (SEJ and RHV), and Grant 4311PT from the Consejo Nacional de Ciencia y Tecnologia (CONACyT) of México (SEJ). We acknowledge the outstanding mapping and observational skills of Jay D. Murray, who completed his Ph.D. studies of the San José pluton in 1978. We extend our sincerest gratitude to the late Aida Meling and her family of the Meling Ranch located on the San José pluton for their hospitality, friendship and assistance over the years: *que ella descanse en paz*. We thank Gary Girty and Brendan McNulty for thorough and constructive reviews of the manuscript, and Jim Evans for editorial assistance.

References

Allison, E.C., 1955. Middle Cretaceous Gastropoda from Punta China, Baja California, México. Journal of Paleontology 29, 400–432.

Allison, E.C., 1964. Geology of areas bordering Gulf of California. In: van Andel, T.H., Shor, G.G., Jr. (Eds.), Marine Geology of the Gulf of California—A Symposium. American Association of Petroleum Geology Memoir 3, pp. 3–29.

Allison, E.C., 1974. The type Alisitos Formation (Cretaceous, Aptian–Albian) of Baja California and its bivalve fauna. In: Gastil, G.,

Lillegraven, J. (Eds.), Geology of Peninsular California. American Association of Petroleum Geologists, Pacific Section, Guidebook to 49th Annual Meeting, pp. 20–59.

Bateman, P.C., 1992. Plutonism in the Central Part of the Sierra Nevada Batholith, California. United States Geological Survey Professional Paper 1483, 186.

Bateman, R., 1984. On the role of diapirism in the segregation, ascent and final emplacement of granitoids. Tectonophysics 10, 211–231.

Bateman, R., 1985. Aureole deformation by flattening around a diapir during in-situ ballooning: the Cannibal Creek granite. Journal of Geology 93, 293–310.

Bridgewater, D., Sutton, J., Watterson, J., 1974. Crustal downfolding associated with igneous activity. Tectonophysics 21, 57–77.

Brun, J.P., Pons, J., 1981. Strain patterns of pluton emplacement in crust undergoing non-coaxial deformation, Sierra Morena, southern Spain. Journal of Structural Geology 3, 219–230.

Brun, J.P., Gapais, D., Cogne, J.P., Ledru, D., Vigneresse, J.L., 1990. The Flamanville granite (NW France): an unequivocal example of a syntectonically expanding pluton. Journal of Geology 25, 271–286.

Busby, C., Smith, D., Morris, W., Fackler-Adams, B., 1998. Evolutionary model for convergent margins facing large ocean basins: Mesozoic Baja California, México. Geology 26, 227–230.

Chavez, G., 1998. Ascent mechanisms, emplacement and magmatic evolution of various plutons west of the Sierra San Pedro Mártir, Baja California, México. Unpublished MSc Thesis, CICESE, Ensenada, México, 165pp.

Courrioux, G., 1987. Oblique diapirism: the Criffel granodiorite/granite zoned pluton (southwest Scotland). Journal of Structural Geology 9, 313–330.

Cruden, A.R., 1990. Flow and fabric development during diapiric rise of magma. Journal of Geology 98, 681–698.

Cruden, A.R., 1998. On the emplacement of tabular granites. Journal of the Geological Society of London 155, 853–862.

DePaolo, D.J., 1981. A Neodymium and Strontium isotopic study of the Mesozoic calc-alkaline granitic batholiths of the Sierra Neveda and Peninsular Ranges, California. Journal of Geophysical Research 86, 10470–10488.

Gastil, R.G., Phillips, R.P., Allison, E.C., 1975. Reconnaissance geology of the State of Baja California. Geological Society of America Memoir 140, 170.

Gastil, R.G., Morgan, G.J., Krummenacher, D., 1978. Mesozoic history of peninsular California and related areas east of the Gulf of California. In: Howell, D.G., McDougall, K.A. (Eds), Mesozoic Paleogeography of the Western United States. Pacific Section, Society of Economic Paleontologists and Mineralogists, Pacific Coast Paleogeography Symposium 2, pp. 107–115.

Gastil, R.G., Morgan, G.J., Krummenacher, D., 1981. The tectonic history of peninsular California and adjacent México. In: Ernst, W.G., (Ed.), The Geotectonic Development of California (Rubey Volume I), Prentice-Hall, Englewood Cliffs, New Jersey, pp. 284–306.

Glazner, A.F., 1994. Foundering of mafic plutons and density stratification of continental crust. Geology 22, 435–438.

Glazner, A.F., Miller, D.M., 1998. Late-stage sinking of plutons. Geology 25, 1099–1102.

Griffith, R., Hoobs, J., 1993. Geology of the southern Sierra Calamajue, Baja California Norte, México. In: Gastil, R.G., Miller, R.H. (Eds), The Prebatholithic Stratigraphy of Peninsular California. Geological Society of America Special Paper 279, pp. 43–60.

Holder, M.T., 1979. An emplacement mechanism for post-tectonic granites and its implications for their geochemical features. In: Atherton, M.P., Tarney, J. (Eds.), Origin of Granite Batholiths, Geochemical Evidence, Shiva, Orpington, Kent, UK, pp. 116–128.

Ichinose, G., Day, S.M., Magistrale, H., Prush, T., Vernon, F.L., Edelman, A., 1996. Crustal thickness variations beneath the Peninsular Ranges, southern California. Geophysical Research Letters 23, 3095–3098.

Johnson, S.E., Paterson, S.R., Tate, M.C., 1999a. Structure and emplacement history of a multiple-center, cone-sheet-bearing ring complex: the Zarza Intrusive Complex, Baja California, México. Geological Society of America Bulletin 111, 607–619.

Johnson, S.E., Tate, M.C., Fanning, C.M., 1999b. New geologic mapping and SHRIMP U–Pb zircon data in the Peninsular Ranges batholith, Baja California, México: evidence for a suture? Geology 27, 743–746.

Johnson, S.E., Albertz, M., Paterson, S.R., 2001. Growth rates of dike-fed plutons: are they compatible with observations in the middle and upper crust? Geology 29, 727–730.

Lagarde, J.L., Brun, J.P., Gapais, D., 1990. Formation of epizonal granitic plutons by in-situ assemblage of laterally expanding magma. C.R. Academy of Science Paris 310 (II), 1109–1114.

Ludwig, K.R., 1999. User's manual for Isoplot/Ex, Version 2.10. A geochronological toolkit for Microsoft Excel. Berkeley Geochronology Center Special Publication No. 1a, 2455 Ridge Road, Berkeley CA 94709, USA.

Ludwig, K.R., 2000. SQUID 1.00. A User's Manual. Berkeley Geochronology Center Special Publication No. 2, 2455 Ridge Road, Berkeley, CA 94709, USA.

Miller, R.B., Paterson, S.R., 1999. In defense of magmatic diapirs. Journal of Structural Geology 21, 1161–1173.

Morgan, S.S., Law, R.D., Nyman, M.W., 1998. Laccolith-like emplacement model for the Papoose Flat pluton based on porphyroblast-matrix analysis. Geological Society of America Bulletin 110, 96–110.

Murray, J.D., 1978. The structure and petrology of the San José pluton, northern Baja California, México. Unpublished Ph.D. thesis. Pasadena, California Institute of Technology, 709pp.

Murray, J.D., 1979. Outlines of the structure and emplacement history of a tonalite pluton in the Peninsular Ranges batholith, Baja California, México. In: Abbott, P.L., Todd, V.R. (Eds.), Mesozoic Crystalline Rocks; Peninsular Ranges Batholith and Pegmatites; Point Sal Ophiolite, San Diego State University, San Diego, California, pp. 163–176.

Nelson, C.A., Sylvester, A.G., 1971. Wallrock decarbonation and forcible emplacement of Birch Creek pluton, southern White Mountains, California. Geological Society of America Bulletin 82, 2891–2904.

Paces, J.B., Miller, J.D., 1993. Precise U–Pb ages of Duluth Complex and related mafic intrusions, northeastern Minnesota: geochronological insights to physical, petrogenetic, paleomagnetic, and tectonomagmatic process associated with the 1.1 Ga Midcontinent Rift System. Journal of Geophysical Research 98, 13,997–14,013.

Paterson, S.R., 1988. Cannibal Creek granite: post-tectonic "ballooning" intrusion or pre-tectonic piercement diapir? Journal of Geology 96, 730–736.

Paterson, S.R., Fowler, T.K. Jr, 1993. Re-examining pluton emplacement processes. Journal of Structural Geology 15, 191–206.

Paterson, S.R., Vernon, R.H., 1995. Bursting the bubble of ballooning plutons: a return to nested diapirs emplaced by multiple processes. Geological Society of America Bulletin 107, 1356–1380.

Paterson, S.R., Vernon, R.H., Tobisch, O.T., 1989. A review of criteria for the identification of magmatic and tectonic foliations in granitoids. Journal of Structural Geology 11, 349–363.

Paterson, S.R., Brudos, T., Fowler, T.K. Jr, Carlson, C., Bishop, K., Vernon, R.H., 1991. Papoose Flat pluton: forceful expansion or post-emplacement deformation? Geology 19, 324–327.

Phillips, J.R., 1993. Stratigraphy and structural setting of the mid-Cretaceous Olvidada Formation, Baja California Norte, México. In: Gastil, R.G., Miller, R.H. (Eds.), The Prebatholithic Stratigraphy of Peninsular California. Geological Society of America Special Paper 279, pp. 97–106.

Phillips, W.J., 1956. The Criffell–Dalbeattie granodiorite complex. Quarterly Journal of the Geological Society of London 138, 221–239.

Ramsay, J.G., 1989. Emplacement kinematics of a granitic diapir: the Chinamora batholith. Journal of Structural Geology 11, 191–210.

Rangin, C., 1978. Speculative model of Mesozoic geodynamics, central Baja California to northeastern Sonora (México). In: Howell, D.G., McDougall, K.A. (Eds.), Mesozoic Paleogeography of the Western United States. Pacific Section, Society of Economic Paleontologists and

Mineralogists, Pacific Coast Paleogeography Symposium 2, pp. 85–106.

Saleeby, J.B., 1990. Progress in tectonic and petrogenetic studies in an exposed cross-section of young (~100 Ma) continental crust, southern Sierra Nevada, California. In: Salisbury, M.H., Fountain, D.M. (Eds.), Exposed Cross-sections of the Continental Crust, NATO Advanced Studies Institute/Kluwer Academic, Dordrecht, pp. 137–158.

Schmeling, H., Cruden, S.R., Marquart, G., 1988. Finite deformation in and around a fluid sphere moving through a viscous medium: implications for diapiric ascent. Tectonophysics 149, 17–34.

Schmidt, K.L., Paterson, S.R., 2002. A doubly vergent fan structure in the Peninsular Ranges batholith: transpression or local complex flow around a continental margin buttress? Tectonics 21, 141–149.

Siegesmund, S., Becker, J.K., 2000. Emplacement of the Ardara pluton (Ireland): new constraints from magnetic fabrics, rock fabrics and age dating. International Journal of Earth Sciences 89, 307–327.

Silver, L.T., Chappell, B.W., 1988. The Peninsular Ranges batholith: an insight into the evolution of the Cordilleran batholiths of southwestern North America. Royal Society of Edinburgh Transactions 79, 105–121.

Silver, L.T., Stehli, F.G., Allen, C.R., 1963. Lower Cretaceous pre-batholithic rocks of northern Baja California, México. American Association of Petroleum Geologists Bulletin 47, 2054–2059.

Stein, E., Paterson, S.R., 1996. Country rock displacement during emplacement of the Joshua Flat pluton, White–Inyo Mountains, California. In: Oncked, O., Janssen, C. (Eds.), Basement Tectonics 11, pp. 35–49.

Sylvester, A.G., Oertel, G., Nelson, C.A., Christie, J.M., 1978. Papoose Flat pluton: a granitic blister in the Inyo Mountains, California. Geological Society of America Bulletin 89, 1205–1219.

Tate, M.C., Johnson, S.E., 2000. Origins of voluminous tonalite in the Méxican Peninsular Ranges and other Cordilleran batholiths. Journal of Geology 108, 721–728.

Tate, M.C., Norman, M.D., Johnson, S.E., Fanning, C.M., Anderson, J.L., 1999. Generation of Tonalite and Trondhjemite by Subvolcanic Fractionation and Partial Melting in the Zarza Intrusive Complex, western Peninsular Ranges batholith, northwestern Mexico. Journal of Petrology 40, 983–1010.

Thompson, C.N., Girty, G.H., 1994. Early Cretaceous intra-arc ductile strain in Triassic–Jurassic and Cretaceous continental margin arc rocks, Peninsular Ranges, California. Tectonics 13, 1108–1119.

Todd, V.R., Shaw, S.E., 1985. S-type granitoids and an I–S line in the Peninsular Ranges batholith, southern California. Geology 13, 231–233.

Todd, V.R., Erskine, B.G., Morton, D.M., 1988. Metamorphic and tectonic evolution of the Peninsular Ranges batholith. In: Ernst, W.G., (Ed.), Metamorphism and Crustal Evolution of the Western United States (Rubey Volume VII), Prentice-Hall, Englewood Cliffs, New Jersey, pp. 894–937.

Vernon, R.H., 2000. Review of microstructural evidence of magmatic and solid-state flow. Electronic Geosciences 5, 2.

Vernon, R.H., Paterson, S.R., 1993. The Ardara granite, Ireland: deflating an expanded intrusion. Lithos 31, 17–31.

Vernon, R.H., Etheridge, M.A., Wall, V.J., 1988. Shape and microstructure of microgranitoid enclaves: indicators of magma mingling and flow. Lithos 22, 1–11.

Walawender, M.J., Girty, G.H., Lombardi, M.R., Kimbrough, D.L., Girty, M.S., Anderson, C., 1991. A synthesis of recent work in the Peninsular Ranges batholith. In: Walawender, M.J., Hanan, B.B. (Eds.), Geological Excursions in Southern California and México, Department of Geological Sciences, San Diego State University, San Diego, California, pp. 297–312.

Weinberg, R.F., Podladchikov, Y.Y., 1995. The rise of solid-state diapirs. Journal of Structural Geology 17, 1183–1195.

Wiebe, R.A., Collins, W.J., 1998. Depositional features and stratigraphic sections in granitic plutons: implications for the emplacement and crystallization of granitic magma. Journal of Structural Geology 20, 1273–1289.

Williams, I.S., 1998. U–Th–Pb geochronology by ion microprobe. In: McKibben, M.A., Shanks III, W.C., Ridley, W.I. (Eds.), Applications of Microanalytical Techniques to Understanding Mineralizing Processes. Reviews in Economic Geology 7, pp. 1–35.